RESEARCH PROGRAMME

BELGIAN SCIENCE POLICY

Bilateral Cooperation

Bilateral Agreement with China

FINAL REPORT

2011-2013

Proposal's title: **Impact of Biogenic Emissions on Beijing Air Quality and Climate**
Proposal's acronym: **IBBAC**
Contract no: ***BL/35/C60***

For the PARTNERSHIP: the coordinator

Dr. Michel Van Roozendael (BIRA-IASB)

DATE: 1 April 2014

Table of Contents

SAMENVATTING

Bilaterale BEL-China R&D samenwerking - BL /35/60

IBBAC

(Impact van biogene emissies op de luchtkwaliteit en het klimaat van Beijing)

Titel : Impact van biogene emissies op de luchtkwaliteit en het klimaat van Beijing

Studiegebied : Beijing, Volksrepubliek China

Doelstellingen en belangrijkste bevindingen

Door zijn hoge bevolking en zijn snelle economische groei behoort Beijing tot de meest vervuilde steden ter wereld. Naast de stijgende vraag naar betrouwbare antropogene emissieschattingen, zijn accurate schattingen van biogene emissies van groot belang in de aanpak van verschillende milieuvraagstukken, zoals de afnemende luchtkwaliteit en de opwarming van de aarde. Het doel van het IBBAC-project was om de rol en de impact van biogene VOS-emissies op de luchtvervuiling tijdens de zomer in de omgeving van Beijing te evalueren. Onder de biogene VOS is isopreen de meest uitgestoten stof en vormt dus de focus van dit werk.

We onderzochten de jaarlijkse variabiliteit van de isopreenuitstoot in China tussen 1979 en 2012 met behulp van het MEGAN-emissiemodel, gecombineerd met het MOHYCAN-bladerdak-omgevingsmodel. Veranderingen in isopreenuitstoot veroorzaakt door de opwarming van het klimaat, de veranderende zonnestraling en de omzetting van primaire bossen in akkerland werden onderzocht. De temperatuur, de zonnestraling en het bodemvocht blijken de belangrijkste drijvende parameters te zijn in de interjaarlijkse variabiliteit in isopreenuitstoot. De gemiddelde opwarming in China (0,3°C per decennium) is de belangrijkste oorzaak voor de berekende toename van isopreenuitstoot, geschat op 0,52 % per jaar. Daarenboven blijken de afnemende akkerbouw en verhelderende zonnestraling de emissietrend te versterken (tot 0,72 % per jaar). In de omgeving van Beijing is de emissietrend van 0,7% per jaar eveneens vooral te wijten aan het opwarmende klimaat.

De samenwerking tussen het BIRA en IAP-CAS maakte MAX-DOAS-metingen mogelijk van de belangrijkste verontreinigende stoffen (NO_2, HCHO, SO_2, HONO en aerosolen) in het centrum van Beijing en op een nabijgelegen suburbane locatie. Deze metingen, aangevuld met satellietwaarnemingen, werden gebruikt om de modelprestaties te evalueren voor een referentiejaar (2008) en een "klimaatveranderingsjaar" (2007).

Met behulp van satellietkolommen van HCHO en geavanceerde inverse modelleringstools, hebben we “top-down” antropogene en pyrogene emissieschattingen afgeleid. We toonden aan dat de pyrogene uitstoot afkomstig van akkerbranden in de Noord-Chinese Vlakte in juni een belangrijke bron van luchtvervuiling blijkt te zijn, die kan concurreren met de emissies van de industrie- en transportsector. Deze emissiebron wordt momenteel verwaarloosd in atmosferische modellen.

Simulaties met het globale IMAGESv2/BIRA-IASB-model en het AURORA/VITO-model met een fijne resolutie, leiden tot kwalitatief vergelijkbare conclusies aangaande de impact van de isopreenuitstoot op de luchtkwaliteit in de buurt van Beijing. Warmere temperaturen en bijgevolg hogere biogene isopreenuitstoot leiden tot een aanzienlijke toename van de gesimuleerde oppervlakteozonconcentraties (ongeveer 20 g/m^3 in de zomer) als gevolg van de zeer hoge stikstofoxidenconcentraties. Dit resultaat benadrukt de nood aan een accurate kwantificatie van isopreenemissies om het beleid gericht op de verbetering van de luchtkwaliteit in deze regio te ondersteunen. Wij adviseren om de samenwerking met Chinese wetenschappers te verbeteren om de belangrijke rol van biogene VOS te bevestigen aan de hand van bijkomende in-situmetingen en modelleringsactiviteiten.

RESUME

Collaboration bilatérale BEL-China R&D - BL /35/60

IBBAC

(Impact des émissions biogéniques sur la qualité de l'air et le climat à Pékin)

Titre : Impact des émissions biogéniques sur la qualité de l'air et le climat à Pékin

Région d'étude : Pékin, République Démocratique de Chine

Objectifs et résultats

De par sa forte population et sa croissance économique rapide, Pékin compte parmi les villes les plus polluées du monde. Outre la demande pressante d'estimations fiables des émissions anthropiques, l'évaluation des émissions par la biosphère et de leur impact sur la pollution de l'air est importante afin de mieux cerner les problèmes majeurs que sont la détérioration de la qualité de l'air et le changement climatique. Le but du projet IBBAC est l'évaluation de l'impact des émissions de composés organiques volatils (COV) biogéniques sur la pollution de l'air à Pékin et dans ses environs. Parmi les COV biogéniques, l'isoprène est le plus largement émis et est donc le principal centre d'intérêt de ce projet.

Nous avons étudié la variabilité des émissions d'isoprène en Chine entre 1979 et 2012, grâce au modèle d'émission MEGAN combiné au modèle de canopée MOHYCAN. Les perturbations des émissions induites par le réchauffement climatique, la variation de l'ensoleillement, et la conversion de forêts en cultures ont été déterminées. La température, le rayonnement solaire et l'humidité du sol s'avèrent être les principaux paramètres gouvernant la variabilité interannuelle. Le réchauffement moyen en Chine (0.3°C par décade) est la principale cause de l'augmentation des émissions, estimée à 0.52% par an, tandis que l'abandon de cultures et l'accroissement de l'ensoleillement renforcent la tendance à l'augmentation (0.72%/an). A Pékin, la croissance est de 0.7% par an, principalement à cause du réchauffement.

La collaboration entre BIRA-IASB et IAP-CAS a permis la mesure de polluants-clés (NO_2, HCHO, SO_2, HONO et les aérosols) par la technique MAX-DOAS à Pékin et dans un site suburbain proche. Ces mesures, en complément d' observations par satellite fournies par BIRA-IASB, ont été utilisées pour évaluer les performances des modèles pour une année de référence (2008) et une année au climat sensiblement différent, l'année 2007.

Grâce aux données de formaldéhyde par satellite et à des techniques poussées d'inversion des sources, nous avons fourni de nouvelles estimations des émissions dues aux activités industrielles et aux feux de végétation. Nous avons démontré que les émissions dues aux feux de résidus agricoles est une source importante de pollution dans la Plaine de Chine de Nord en juin, de magnitude comparable aux émissions anthropiques. Cette source est actuellement ignorée dans les modèles.

Des simulations du modèle global IMAGESv2/BIRA-IASB et du modèle à haute résolution AURORA/VITO ont conduit à des conclusions similaires concernant l'impact des émissions d'isoprène sur la qualité de l'air dans la région de Pékin. Le réchauffement et les émissions accrues qui en résultent apparaissent comme la cause d'une augmentation substantielle des concentrations d'ozone en été, d'environ 20 $\mu g/m^3$, en raison des fortes abondances d'oxydes d'azote. Ce résultat souligne la nécessité d'une quantification précise des émissions biogéniques afin de guider les politiques visant au contrôle de la qualité de l'air dans cette région. Nous recommandons de renforcer la collaboration avec les équipes chinoises dans le but de confirmer le rôle important des COV biogéniques au moyen de mesures in situ et de nouvelles activités de modélisation.

SUMMARY

Due to its high population and rapid economic growth, Beijing ranks among the most polluted cities worldwide. Besides the rising demand for reliable anthropogenic emission estimates, the evaluation of emissions from the biosphere and their effects on air pollution is very important for addressing environmental issues such as air quality degradation and climate warming. The aim of the IBBAC project was to evaluate the impacts of biogenic VOC emissions on air pollution levels in Beijing and surrounding areas. Among the biogenic VOCs, isoprene is the most largely emitted and is therefore a primary focus of this work.

We have investigated the interannual variability of isoprene emissions in China between 1979 and 2012, using the MEGAN emission model combined with the MOHYCAN canopy model. Changes in isoprene emissions induced by the warming climate, changes in solar radiation, and the conversion of forests to croplands have been explored. Temperature, solar radiation and soil moisture are found to be the main drivers of interannual variability. The average warming trend over China (0.3°C per decade) is the primary cause for the increase in isoprene emissions, estimated at 0.52% per year, whereas crop abandonment and solar brightening are found to reinforce the emission trend (0.72%yr). In Beijing area the emission trend amounts to 0.7% per year, mostly due to the warming climate.

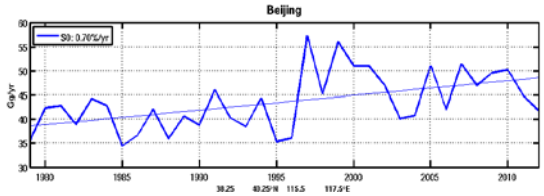

MAX-DOAS UV-Visible measurements of key pollutants (NO_2, HCHO, SO_2, HONO and aerosols) were performed at downtown Beijing (cf. figure on the right) and at the suburban site of Xianghe near Beijing in collaboration between BIRA-IASB and IAP-CAS. These measurements, complemented by satellite observations made available within this project by BIRA-IASB, were used to evaluate the model performances for a reference year (2008) and a "climate-change" year, chosen here to be the exceptionally warm 2007.

Using satellite columns of HCHO and advanced inverse modelling tools, we have derived top-down anthropogenic and biomass burning emission estimates. We showed that fire emissions in the North China Plain in June related to harvest season burning is an important source of pollution competing with the emissions from the industrial and transport sector. This emission source is currently neglected in atmospheric models.

Simulations of the global model IMAGESv2/BIRA-IASB and the fine resolution AURORA/VITO model led to qualitatively similar conclusions regarding the impact of isoprene emissions on air quality in the vicinity of Beijing. Warmer temperatures and the resulting higher biogenic isoprene emissions are found to cause a substantial increase in the surface ozone summertime concentrations, by around 20 µg/m^3, as a result of the very high nitrogen

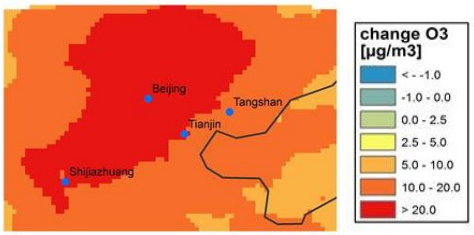

oxides concentrations. This result emphasizes the need for an accurate quantification of isoprene emissions in order to guide policy making aiming at the mitigation of air quality in this region. We recommend to enhance collaboration with Chinese teams in order to confirm the important role of biogenic VOC by means of in situ measurements and further modelling activities.

OVERALL APPRECIATION OF THE COLLABORATION – VALORIZATION EFFORTS

A major asset of IBBAC is the longstanding expertise of the partners in both measurement and modelling activities. At first place, the MAX-DOAS atmospheric measurements obtained within IBBAC in close collaboration with the Chinese partner, the Institute for Atmospheric Physics (IAP) of the Chinese Academy of Sciences, at two sites, downtown Beijing and at the suburban site of Xianghe, is a valuable and unique dataset covering almost six years of measurements. The instrument, assembled at BIRA-IASB, allowed to acquire high quality measurements of NO_2, HCHO, SO_2, HONO and aerosols, by virtue of its high signal-to-noise ratio in both ultraviolet and visible spectral windows. These measurements, complemented by satellite observations of trace gases like HCHO and NO_2 obtained from the UV-Vis retrieval team of BIRA-IASB, are decisive tools for air quality assessments in the Beijing agglomeration. They further capitalize the Belgian expertise abroad, stimulate research and help to define policy directions, as testified by the large number of publications and presentations in international fora.

An additional asset within IBBAC has been the close collaboration between BIRA-IASB and VITO which allowed to take advantage of their respective experience on state-of-art numerical models, namely, the IMAGES global tropospheric model developed at BIRA-IASB and the AURORA high resolution air quality model developed at VITO. The combination of coarse and fine resolution models for air quality assessment brings valuable insight in the underlying processes controlling the current air quality status.

However, owing to the change of affiliation in the course of the first year of the project of Professor Zifa Wang, who was in charge for the modelling activity on the Chinese side, a deviation from the initial plan could not be avoided. This task has not been taken over by another member of the IAP modelling group, however, mostly because of the lack of funding of the Chinese part through the MOST mechanism. In an effort to collaborate with another modelling group, we established contact with Professor Jintai Lin from Peking University, world-wide expert in atmospheric and air pollution modeling. Although the participation of Professor Lin and his group in IBAAC has not been possible within the tight IBBAC deadlines and given its voluntary basis, he and his group will be glad to collaborate with us in the framework of a similar bilateral initiative in the future.

An important contribution in IBBAC was the quantification of biogenic emissions over China, thanks to the expertise of BIRA-IASB in the development of emission models. The study of emission trends due to the warming climate and land use changes, performed within IBBAC, has attracted a lot of attention from other research groups in China, interested to use these estimates in their models and for validation purposes.

To put a figure on both the direct and the more long-term benefits of IBBAC for the Belgian partners, we highlight

i. the participation of BIRA-IASB and VITO in the European Collaborative project FP7-EC606953 "*Monitoring and Assessment of Regional air quality in China using space Observations, Project of Long-term sino-european Co-operation*- MARCOPOLO", which started on January 2014 and will run for 3 years;

ii. the current collaboration with Professor Qiang Zhang from the Tsinghua University who developed and provided access to the Multi-Resolution Emission Inventory for China (MEIC), now implemented in IMAGESv2 model;

iii. the invitation to be part of the expert panel in the "*2013 China Emission Workshop*", organized by Tsinghua University in Beijing (26-27 June 2013), addressed to policy makers in China (*EA2 Initiative*). IBBAC project has thus tangibly contributed in raising awareness on the role of biogenic VOC emissions in atmospheric pollution in China, and the associated impact on policy measures targeting improved air quality in Beijing megacity;

iv. the further development of synergies on measurement campaigns and modelling studies, extension and reinforcement in the future through new contacts established in the IBBAC progress meeting, organized at IAP in 2012 (cf. Annexe for more details) and through the FP7-MARCOPOLO opportunities;

Last but not least, the large number of publications (9 published, 3 in preparation), and oral presentations (11, among which 4 invited) presented in international conferences and workshops demonstrate the large valorization effort undertaken within IBBAC (cf. Annexes). In addition, in the project webpage (http://tropo.aeronomie.be/ibbac), hosted by BIRA-IASB, one can find details about the tasks, the valorization efforts and password-protected documents (login: IBBAC, password: IBBACusers) such as previous reports and presentations.

ADMINISTRATIVE REPORT

FOR PARTNER 1, BELGIAN INSTITUTE FOR SPACE AERONOMY

Modifications to the contract: Contract extended until end of 2013

List of personnel working on the project (in charge of the project or not):

Personnel working on the project, funded by the budget:

Name	Title/function
Maite Bauwens	Scientist, +3223730421, maite.bauwens@aeronomie.be
Yu Huan	Scientist, +3223730405, huan.yu@aeronomie.be

Personnel working on the project, not funded by the budget :

Name	Title/function
Michel Van Roozendael	Coordinator, Senior scientist +3223730416, michelv@aeronomie.be
Jenny Stavrakou	Co-promotor, Scientist +3223736766, jenny@aeronomie.be
Jean-François Müller	Senior scientist, +3223730366, jfm@aeronomie.be
Isabelle De Smedt	Scientist, +3223730407, isad@aeronomie.be

Overview of performed tasks regarding each workpackage:

WP1 : Biogenic emission estimates over Northeastern China

- Derivation of a historical (1979-2012) biogenic emission record for China based on the MEGAN emission model and ECMWF meteorological fields
- Determination of a year with exceptionally hot summer, to be termed as reference for a "climate change" case
- Improved representation in the IMAGESv2 model of biogenic and anthropogenic VOCs of importance for China, based on recent speciation data for anthropogenic VOCs
- Derivation of improved emission estimates for reactive VOCs using IMAGESv2 in an inversion setup constrained by HCHO columns from the GOME-2 instrument

WP2 : Model/data intercomparisons – present and "climate-change" model simulations

- MAX-DOAS measurements of NO_2 and HCHO at Beijing and Xianghe performed through the collaboration between BIRA-IASB and IAP
- Comparisons with the IMAGESv2 model columns of HCHO before and after optimization
- Provide IMAGESv2 output concentration fields at the lateral boundaries, as well as top-down VOC emissions for summer 2007 and 2008, to AURORA/VITO model at http://tropo.aeronomie.be/ibbac/data.html
- Evaluation of the impact of biogenic emissions and the impact of meteorology on the concentrations of pollutants and oxidants for the 'climate change'-like year 2007 and for the reference year 2008.

FOR PARTNER 2, FLEMISH INSTITUTE FOR TECHNOLOGICAL RESEARCH (VITO)

Modifications to the contract: Contract extended until end of 2013

List of personnel working on the project (in charge of the project or not):

Personnel working on the project, funded by the budget:

Name	Title/function
Peter Viaene	Researcher, +32-14336744, peter.viaene@vito.be

Personnel working on the project, not funded by the budget :

Name	Title/function
Koen De Ridder	Co-promotor, Senior scientist +32-14335968, koen.deridder@vito.be
Lisa Blyth	Project Manager, +3214336757, lisa.blyth@vito.be
Nele Veldeman	Researcher, +32 14 33 67 46, nele.veldeman@vito.be

Overview of performed tasks regarding each workpackage:

WP1 : Biogenic emission estimates over Northeastern China

- Downscaling of the biogenic emission estimates derived for northeastern China provided by BIRA-IASB
- Implementation of the top-down anthropogenic, pyrogenic and biogenic emissions in the AURORA/VITO model

WP2 : Model/data intercomparisons – present and "climate-change" model simulations

- Implementation of IMAGESv2 lateral conditions in the AURORA/VITO model, so as to account for long-range pollutant transport
- Comparison of AURORA/VITO model to measurements of MAX-DOAS NO_2 and HCHO performed at Beijing and Xianghe for the reference year 2008
- Model results for the reference year 2008 and the 'climate-change'-like year 2007
- Investigation of the effects of boundary conditions, meteorology and biogenic emissions on surface ozone concentrations, NO, NO_2, peroxyacetyl nitrate (PAN), HNO_3, $PM_{2.5}$, ammonium 2.5, nitrate 2.5, and sulphate 2.5.

SCIENTIFIC REPORT

1. CONTRIBUTION OF BIRA-IASB IN WP1

1.1 BOTTOM-UP ISOPRENE EMISSION INVENTORY FOR CHINA

Due to the scarcity of observational constraints and the rapidly changing environment in East Asia, isoprene emissions predicted by models are expected to bear substantial uncertainties. The aim here is to improve upon the existing bottom-up estimates, and investigate the temporal evolution of the fluxes in Asia over 1979–2012. To this purpose, we calculate the hourly emissions at 0.5×0.5 degree resolution using the MEGAN-MOHYCAN model driven by ECMWF ERA-Interim climatology. In this framework we incorporate (i) changes in land use, (ii) meteorological variability according to ERA-Interim, (iii) long-term changes in solar radiation (dimming/brightening) constrained by surface network radiation measurements, and (iv) recent experimental evidence that tropical forests are much weaker isoprene emitters than previously assumed.

Within IBBAC, we perform a baseline simulation of isoprene emissions using the MEGAN-MOHYCAN model (S0 simulation) described in Guenther et al. (2006) and Müller et al. (2008) through 1979-2012. The simulation accounts for the effects of climate change according to ERA-Interim data. In simulation S1 (Table 1), the static land use cropland map used in MEGAN is replaced by the vegetation map of Ramankutty and Foley (1999) to account for the effect of land use changes (Figure 1). According to this database, significant cropland abandonment is widespread in Central and South China, mostly due to urbanization, as well to the conversion of crops to tree plantations for economic reasons (e.g. Eucalyptus and rubber tree).

The S2 simulation accounts for the recent evidence that emissions of isoprene from tropical forests are likely to be overestimated in the MEGAN model, by as much as a factor of 4, in comparison to above-canopy measurements in Borneo (Langford et al. 2010). This factor is applied to the MEGAN emission rate for all primary tropical forests in the S2 scenario.

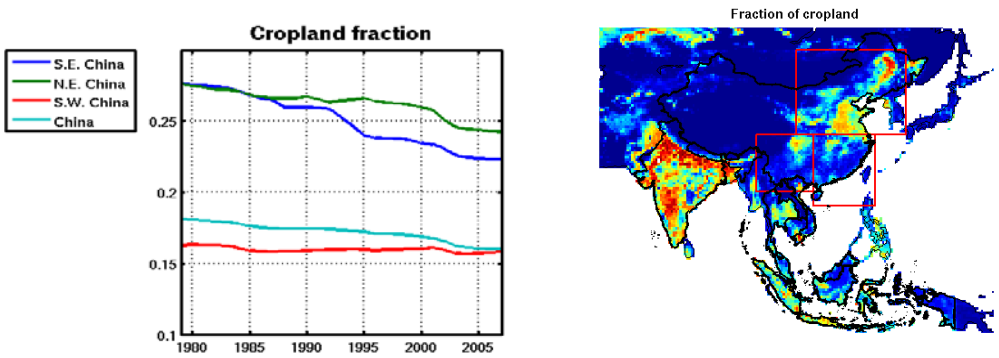

Figure 1. Evolution of cropland fraction over China in 1979-2007 (Ramankutty and Foley, 1999 with updates from http://www.geog.mcgill.ca/nramankutty/Datasets/Datasets.html).

The S3 scenario, which accounts for the impact of oil palm expansion in Malaysia and Indonesia on the isoprene emissions, does not introduce any change to the isoprene emissions in China. The S4 scenario (Table 1) is designed to account for decadal changes in solar radiation fields observed in Asian regions, which the ECFWF analyses cannot reproduce due to their static representation of aerosols (Figure 2). To this purpose, we have used annual surface solar radiation anomaly data observed at several stations in China from Xia (2010) between 1979 and 2005, and calculated correction factors for every year, which are uniformly applied to the photosynthetic flux density. A strong solar dimming was observed in China from 1961 to 1990, especially over eastern China, where surface stations recorded negative trends of about 10 Wm^{-2} per decade. This tendency slowed down after 1990 in Northern China, and even changed sign in Southern China.

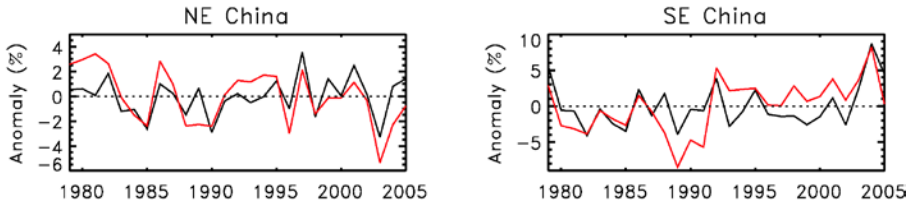

Figure 2. Annual downward surface radiation anomaly (SSR, in %) derived from ERA-Interim fields (black) and corrected based on ground-based SSR observations in Northeastern and Southeastern China (Xia, 2010).

Table 1. Bottom-up scenarios for calculating isoprene emissions.

Name	Description
S0	MEGAN-MOHYCAN, standard settings
S1	as S0, account for land use changes
S2	as S1, emission factor reduction for tropical forests
S3	as S2, changing oil palm plantations in Indonesia and Malaysia
S4	as S3, correct solar radiation based on network of observations

China experiences a large isoprene flux trend, amounting to 0.52% per year between 1997 and 2012 (Figure 3). The drivers for this trend are the warming rate (0.3°C/decade) and the increasing solar radiation trend (0.3%/decade). The region experiencing the strongest warming trend (0.4-0.6°C/decade) is situated close to Shanghai (Jiangsu, Anhui, and Zhejiang provinces), as well as in the Northern provinces, in agreement with reported data from a large number of weather stations in China. In Southern China, however, the decadal temperature trend is generally lower that 0.4°C/decade and often close to zero, but the radiation trend is larger in this region (1-3%/decade, Figure 4).

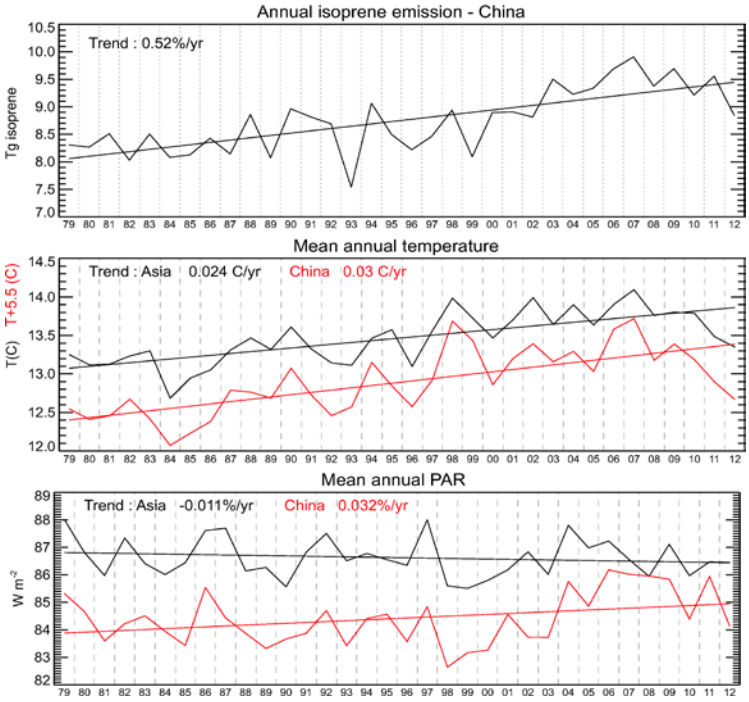

Figure 3. Annual isoprene emissions in China over 1979-2012 calculated by the S0 simulation (Table 1). Annual temperature and photosynthetically active radiation (PAR) is shown over the same period. Linear regression trends are given inset and applied over the whole simulation period.

As illustrated in Figure 4, the spatial patterns of isoprene trends are generally well explained by the spatial distribution of temperature, radiation, and soil moisture trends, suggesting that these variables dominate the behavior of the resulting flux. The largest isoprene trends are apparent at the frontier of Mongolia, China and Russia, where, nevertheless, the isoprene emission capacity is rather weak. Over China, the largest emission flux is calculated by the S0 simulation in 2007, which happens to be the warmest year in our data series, but also a year experiencing high values of solar radiation (Figure 3). Between 2008 and 2012, however, the mean annual temperature declined, resulting in decreasing isoprene fluxes for these years. Therefore, we have chosen year 2007 as 'climate change'-like year, and 2008 as a reference year in our model simulations presented in WP2.

The annual isoprene emission distributions calculated by the different simulation (Table 1) are illustrated in Figure 5 for 2005. The highest emission rates are found in the Southeastern China, whereas emissions in the Northeast are limited by virtue of the lower temperatures and near-zero emission during wintertime from deciduous trees, dominant in this region. The use of cropland database in S1 leads to a 6% flux increase in China, as a result of the cropland abandonment suggested by the land use change database of Ramankutty and Foley (1999). Overall, the impact of solar radiation changes is found to be generally small over China. The annual emission over China is estimated at 7 Tg/yr in the S4 simulation. The isoprene fluxes in the standard S0 simulation in China exhibit an upward annual trend of 0.42%/yr in 1979-2005. This trend is strongly reinforced when adopting the land use changes of the S1 scenario (0.7%/yr), due to the replacement of cropland with tree plantations (Figure 1). Higher emissions are estimated throughout the whole simulation period compared to S0, and especially after 1994. Furthermore, the updated solar radiation changes of S4 simulation lead to an even higher emission trend (0.78%/yr) because of the solar brightening recorded in the isoprene-rich Southeast China (Figure 6). As a consequence of the reduced solar radiation fluxes over China (Jia et al., 2013) adopted in S4 simulation, the emission is further reduced by about 15%

over the whole country. The interannual patterns are quite similar in all simulations, however, changes are also present, e.g. the 1993-1994 peak-to-trough difference is decreased in S4 compared to S0 (Figure 6).

The bottom-up isoprene emissions from S0 simulation have been made available to VITO for downscaling. This will be treated in detail in Section 1.3.

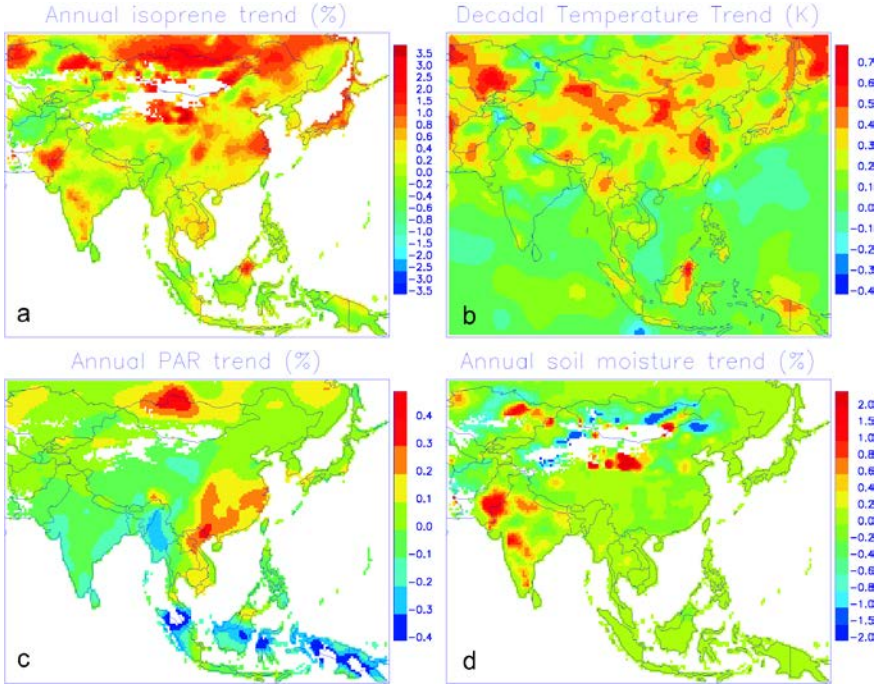

Figure 4. (a) Annual percentage trend in isoprene emissions derived from the S0 simulation over 1979-2012 (Table 1). Decadal temperature trend (b), annual percentage PAR trend (c) and soil moisture trend (d) based on ERA-Interim data over 1979-2012.

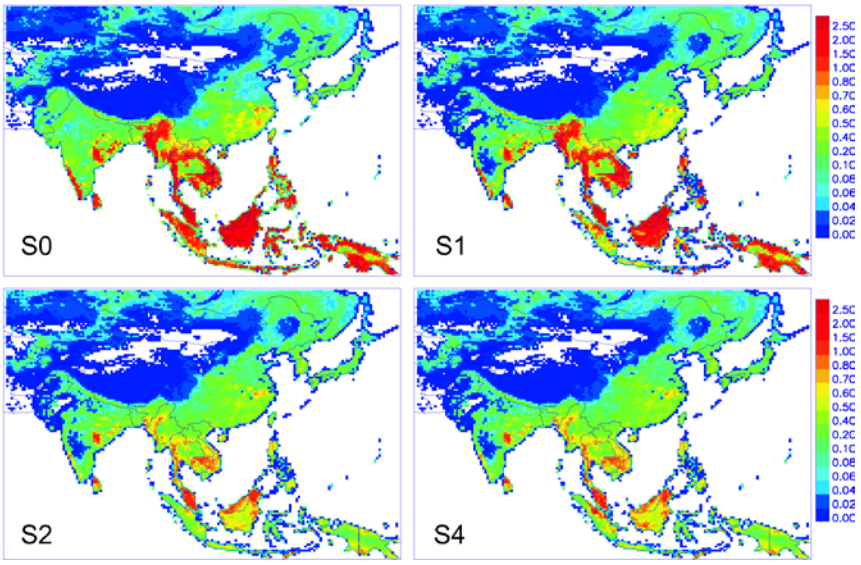

Figure 5. Annually averaged isoprene emission rates computed in S0, S1, S2 and S4 simulation for 2005. S1 accounts for land use change effects, S2 also incorporates reduced emission rates from tropical forests, and S4 includes both updates in solar radiation and in the representation of oil palms in Indonesia and Malaysia (Table 1).

1.2 SETTING UP THE INVERSION OF HCHO COLUMNS

Formaldehyde (HCHO) is a major intermediate product in the degradation of isoprene in the atmosphere. Isoprene is found to be responsible for about 30% of the formaldehyde formed on the global scale, but its contribution over densely vegetated continental areas can be as high as 90%. HCHO vertical column abundances obtained from satellite observations have been used in a number of studies as independent means to constrain the isoprene fluxes, and possibly improve the currently available bottom-up inventories. The capabilities of HCHO columns retrieved from satellite instruments have been explored in several studies aiming to derive isoprene emission estimates over the United States (e.g. Palmer et al. 2003), over China and Southeast Asia (e.g. Fu et al. 2007), on the global scale (Stavrakou et al. 2009), and more recently, over Africa (Marais et al. 2012). In the present study, isoprene emissions over East and South Asia are derived by adopting a grid-based source inversion scheme (Stavrakou et al. 2009a) constrained by a new dataset of HCHO columns measured by the GOME-2/MetOp-A satellite instrument between 2007 and 2012 (De Smedt et al. 2012).

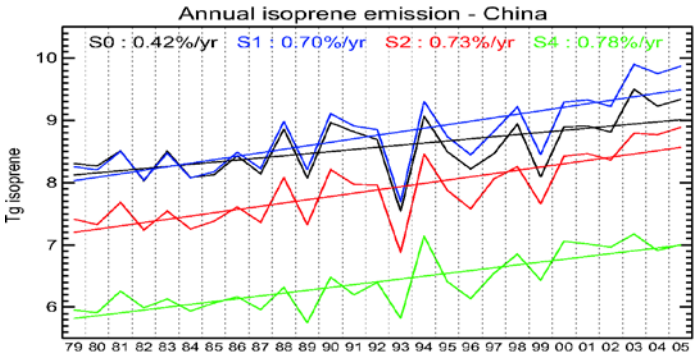

Figure 6. Annual isoprene emission per country between 1979 and 2005. The colors denote different simulations : S0 in black, S1 in blue, S2 in red, S4 in green. Relative trends obtained by linear regression are given inset following the same color code.

The settings adopted for this retrieval were optimised in order to minimise the effect of spectral interferences between HCHO and BrO, to contend with ozone absorption at high solar zenith angles, and to mitigate instrumental drifts, so as to ensure maximum consistency with HCHO columns obtained from earlier sensors (e.g. GOME and SCIAMACHY, De Smedt et al. 2012). HCHO columns and their error characterization are available at the TEMIS website (http://h2co.aeronomie.be). The source inversion is built on the IMAGESv2 (Intermediate Model of Annual and Global Evolution of Species) global chemistry-transport model run at a resolution of 2x2.5 degree and resolved in 40 vertical levels from the surface to the lower stratosphere. Separate inversions are performed for each year from 2007 to 2012. Advection is driven by ERA-Interim fields. The isoprene oxidation chemistry, which recycles OH more efficiently than generally assumed in models under low NOx conditions, follows the LIM0 mechanism (Peeters and Müller, 2010}, with reduced isomerisation rates of isoprene peroxy radicals based on an updated theoretical estimation (Peeters et al., 2012}. Box model calculations show that accounting for the isomerization in the isoprene oxidation reduces the HCHO yield from isoprene by about 10% at both high and low NOx regimes. Nevertheless, the isoprene degradation mechanism is far from being elucidated, especially in low NOx conditions, and therefore, remains a major source of uncertainty when mapping isoprene estimates using HCHO observations.

Anthropogenic NMVOC emissions over Asia are taken from the REASv2 inventory (Kurokawa et al. 2013). Vegetation fire emissions are obtained from GFEDv3 (van der Werf et al. 2010) until

2011 and are set to 2011 values in 2012. The biogenic emissions of isoprene are obtained from S4 for 2007-2011 (Table 1) (i) using the 2007 cropland map for 2008-2012, and the 2010 oil palm distribution for 2011-2012, and (ii) applying only the correction factors for China from Jia et al. 2013 to all years. This dataset of bottom-up emissions spanning 1979-2012 is available for use through http://tropo.aeronomie.be/models/isoprene.htm (MEGAN-ECMWF-v2).

We use monthly averaged GOME-2 HCHO columns binned onto the resolution of IMAGESv2. Observations over ocean and cloudy pixels (i.e. cloud fraction above 20%) are filtered out. The error on the columns is taken equal to the retrieval error augmented by an absolute error of 2x 10^{15} molec.cm^{-2} and is generally comprised between 30-40%. The inversion optimises monthly emission fluxes for three emission categories : anthropogenic, biomass burning and biogenic (isoprene and terpenes). The assumed error on the biogenic emissions is set equal to a factor of 2.5. Here we present only results over Asia. The inversion scheme is shown in Figure 8.

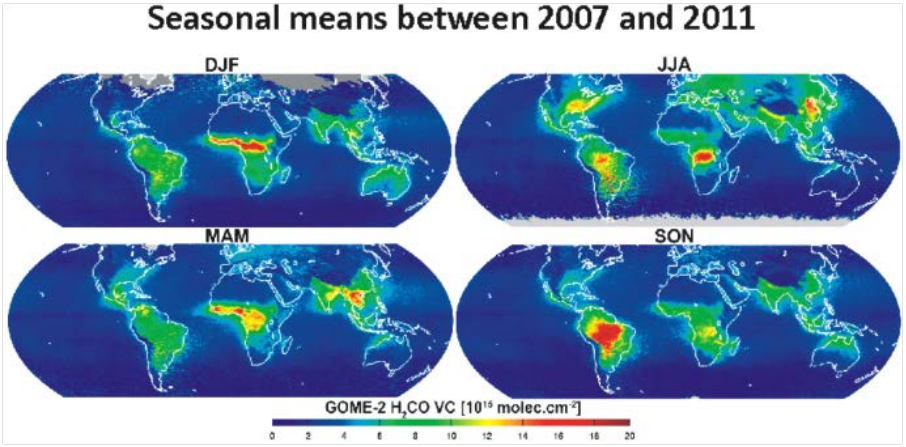

Figure 7. Seasonal means of HCHO columns between 2007 and 2011 (De Smedt et al. 2012).

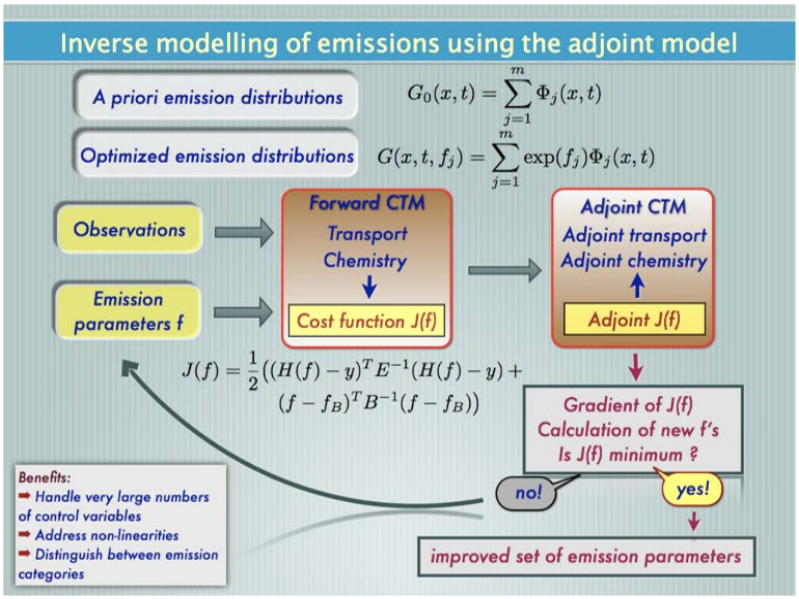

Figure 8. The inversion scheme used in the inversion of HCHO columns.

1.3 TOP-DOWN RESULTS

The inversion updates the anthropogenic VOC emissions, the pyrogenic emissions, as well as the isoprene emissions. In the chemical mechanism of IMAGESv2, the OTHC species represent a mix of anthropogenically emitted VOCs, with lifetime against oxidation by OH optimized so as to reproduce the mean *short-term* and *long-term* yield of HCHO of the mix estimated using the Master Chemical quasi-explicit mechanism (MCM). In the inversion study we use GOME-2 HCHO columns for May and July to infer anthropogenic emissions, June data are omitted in the inversion in a way to minimize interferences from crop fires.

With respect to the REASv2 anthropogenic emission inventory used as a priori in IMAGESv2 global model, the satellite data suggest moderate increases in the Beijing region, and almost no change in the rest of North China Plain. However, emission decreases are inferred in the Southeast China and especially in Pearl River Delta region (up to 30%, Figure 9).

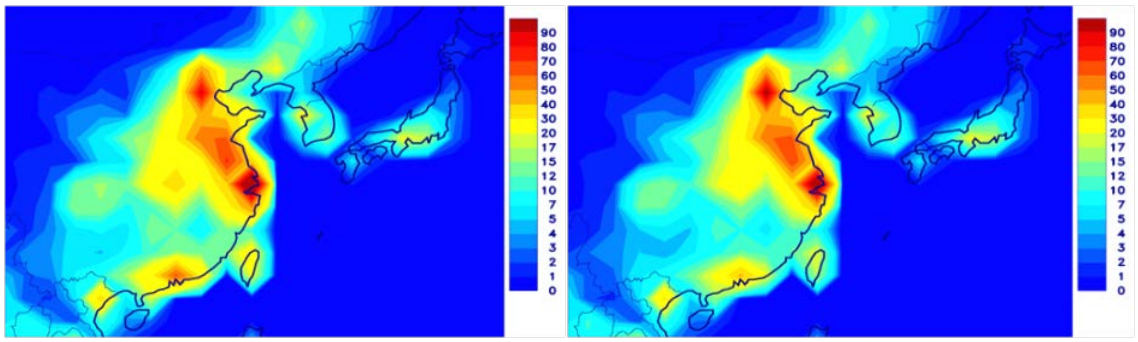

Figure 9. Left : Anthropogenic emissions from the REASv2 inventory in May 2008. Right : Optimised anthropogenic emissions in May 2008 inferred by HCHO columns. Units are 10^{10} molec.cm^{-2} s^{-1}.

As illustrated in Figure 10, the satellite-derived emissions are by about 10% lower than in REASv2 (by ~10%), especially in 2009 and 2010, presumably reflecting economic slowdown and implementation of cleaner technologies. Optimized emissions lie closer to the a priori in 2011. Comparison with the recent MEIC inventory for 2008 (Qiang Zhang, www.meicmodel.org) shows that the top-down estimates lie within the two bottom-up inventories.

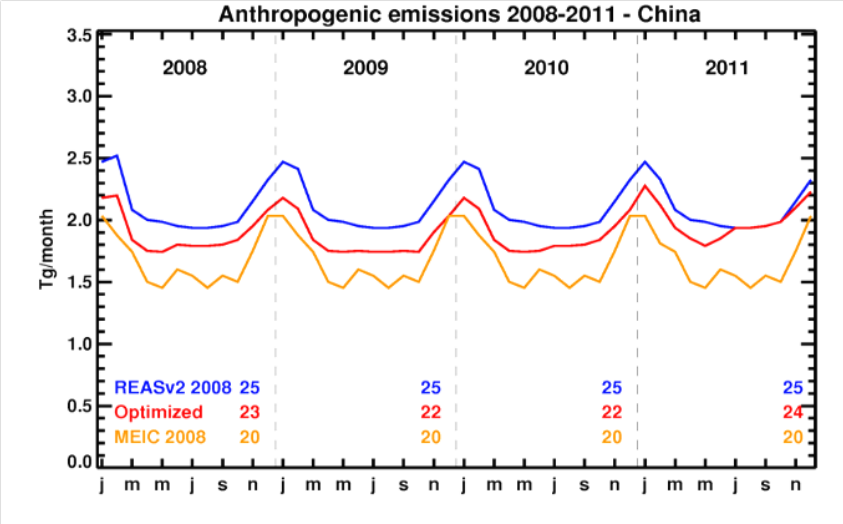

Figure 10. Comparison between a priori REAv2 anthropogenic VOC emissions in China (in blue), optimized emissions (in red), and MEIC 2008 emissions.

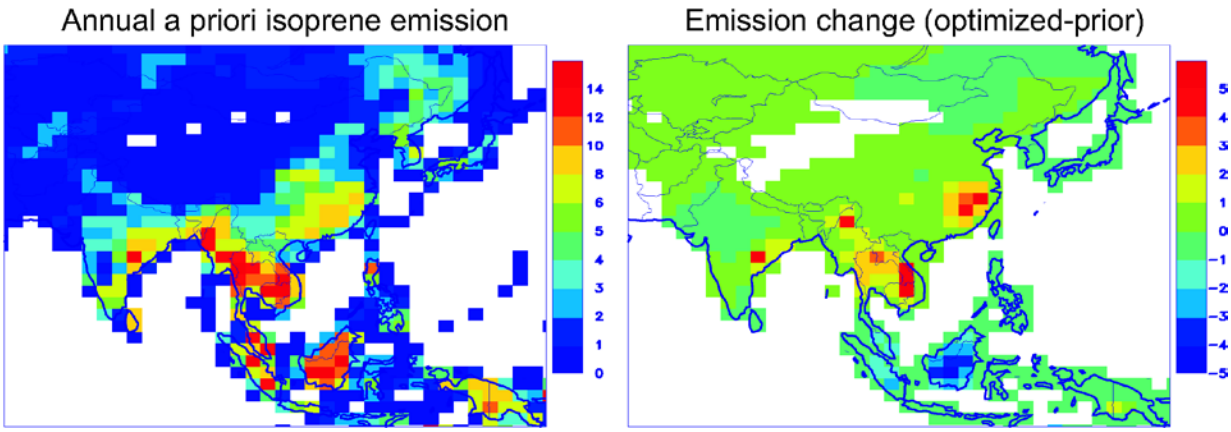

Figure 11. Annual a priori isoprene emission in 2008 and deviation from the a priori. Units are are 10^{10} molec.cm^{-2} s^{-1}. The a priori inventory is obtained from the S4 simulation (Table 1).

Figure 11 displays the spatial distribution of the a priori (bottom-up) isoprene emissions and the deviation from the a priori inferred by the inversion in 2008. The inferred updates with respect to the a priori are generally small over China, except in Southern China where an increase by 30% is deduced in 2008. The inferred changes in Southern China, however, do not exhibit any systematic pattern : they are positive in 2007-2009, close to zero in 2010, and negative in 2011 and 2012.

In conclusion, the bottom-up inventory is partially validated by inverse modelling using formaldehyde as a proxy for VOC emissions. The GOME-2 observations largely support the evidence that tropical rainforests are weaker isoprene emitters than assumed in MEGAN, in particular over Indonesia and Malaysia. Top-down results are very close to the a priori over China. Over China, a significant emission decline is found after 2007 (-25% in 5 years), consistent with the emission decrease of the bottom-up inventory resulting from the cooling trend over China beyond 2007 (Stavrakou et al. 2014).

2. CONTRIBUTION OF VITO IN WP1

2.1 PRODUCTION OF HIGH RESOLUTION EMISSIONS FOR THE AREA OF INTEREST - INTRODUCTION

Among the aims of WP1 was the generation of high resolution emission maps of isoprene. For a chemical transport model (CTM) emissions are needed on the resolution of the model grid. This requires that emissions are spatially distributed taking into account the location of the emitting source(s) and their heights. Emissions also have to be distributed in time. Some emission sources such as those from a continuously operating industrial facility are emitted at a constant rate throughout the year however this is hardly the case for most emissions where the rate could depend on the season (e.g. residential heating) or the time of the day or day of the week (e.g. traffic). To be able to distribute the emissions in time, emissions are typically assigned to sectors where each sector has a particular temporal behaviour. Total emissions are therefore

distributed over individual sectors. Emissions also have to be assigned to the pollutant species that are accounted for in the CTM. For some species such as NH3 there is a direct mapping while others such as non-methane volatile organic compounds (NMVOC) emissions require a reassignment to individual species of the chemical mechanism that is used in the CTM.

To derive high resolution emissions the following procedure was adopted:

- For the anthropogenic NMVOC emissions and the biogenic isoprene emissions the monthly emission totals were constrained using the BIRA-IASB inputs.
- The distribution of the emissions over the sectors and over the pollutant species was based on the information in the MEIC emission inventory for 2008.
- The spatial distribution of the anthropogenic emissions was based on the EDGAR database. For the isoprene emissions results of the MEGAN model were used at the model grid resolution and for the pyrogenic emissions a land use map was used.

This is further explained in the next sections.

2.2 HIGH RESOLUTION ANTHROPOGENIC EMISSIONS

For the NMVOC BIRA-IASB provided emission at a resolution of 0.25° based on inverse modelling for the summer months of 2007 and 2008. Details on these emissions can be found in Section 1.2. These emissions were used to constrain the NMVOC emission totals. To distribute the NMVOC over the different model species needed for the chemistry scheme and also to assign the emissions to different sectors the MEIC inventory version 1.0 for 2008 was used. MEIC (Multi-resolution Emission Inventory for China) was developed at the university of Tsing Hua in Beijing by Professor Qiang Zhang. The inventory can be accessed online (http://www.meicmodel.org/) and includes anthropogenic emissions of China for ten chemical species: SO_2, NOx, CO, NMVOC, NH_3, CO_2, $PM_{2.5}$, PM coarse, BC and OC. Emissions are available for 2008 and 2010 with monthly temporal variation. Gridded emissions are provided with 0.25°, 0.5° and 1° resolution. NMVOC emissions can be downloaded in the individual species that are required for the CB05, SAPRC99, and RADM2 chemical mechanisms. In the case of AURORA we apply the CB05 mechanism with an extension for secondary organic aerosols and the corresponding CB05 MEIC data were therefore used. In our case the BIRA-IASB 0.25° NMVOC emission total were used to scale the MEIC NMVOC emissions. This was done for each of the 3 summer months and two years separately. For SO_2, NOx, CO, NH_3, CO_2, $PM_{2.5}$, PMcoarse, BC and OC the emissions from MEIC were used as such.

To further spatially distribute the emissions, the data in the EDGAR database version 4.2 were used. EDGAR (Emission Database for Global Atmospheric Research) was developed by the European Commission, Joint Research Centre (JRC) and the Netherlands Environmental Assessment Agency (PBL) and can be accessed at edgar.jrc.ec.europa.eu. EDGAR contains data for CH_4, CO, NH_3, NMVOC, NOx, PM_{10} and SO_2 at a resolution of 0.1°. To be able to combine the information in EDGAR with the 0.25° emissions obtained from MEIC, the sectors defined in the EDGAR database were mapped into the corresponding sectors of MEIC as described in Table 1. Using these mappings the EDGAR emissions were merged to the MEIC sectors on the 0.1° grid.

Table 2. Correspondence made between the MEIC sectors and the sectors used in the EDGAR database.

MEIC	EDGAR	
Industry	**1A1+1A2**	Energy manufacturing transformation
	1A1b+1A1c	Refineries and transformation
	1A1b+c+1B+2C1+2C2	Transformation fossil fuel production refineries steel
	1A2	Combustion in manufacturing industry
	1B1	Fugitive from solid
	1B1+1B2+c+1A1b+c	Transformation, Oil production and refinering
	1B2a	Oil production and refineries
	1B2b	Gas production and distribution
	2	Industrial process and product use
	2+3	Process emissions during production and application
	2A	Non-metallic mineral processes
	2A+2B+2D	Non-metallic paper chemical industry
	2A+2B+2D+2E+2F+2G	Non-metallic paper chemical food industry
	2B	Chemical industry
	2C	Metal processes
	3	Solvents production and application
Energy	**1A1a**	Energy industry
	1A1a+6C	Energy industry and waste incinerator
Transport	**1A3**	Transport non-road and road
	1A3a+c+d+e	Non-road transportation
	1A3b	Road transportation
Residential	**1A4**	Residential
Agriculture	**4A**	Enteric fermentation
	4B	Manure management
	4C+4D	Agricultural soils
	4F	Agricultural waste burning
	5A+C+D+F+4E	Large scale Biomass burning
	6A+6C	Solid waste disposal
	6B	Waste water
	7A	Fossil fuel fires

An analysis between the EDGAR and MEIC emission totals for the model area for the MEIC sectors revealed some marked differences between both databases (Table 3). For some sectors there are apparently no corresponding emissions in both inventories. To cope with this, the EDGAR emissions were modified proportionally to the emissions of the overlapping MEIC-cells (**Figure 1**2) when there were emissions according to both inventories. If this was not the case, the MEIC emissions were homogeneously distributed over the corresponding EDGAR-cells.

Table 3. Total of emissions in the model area (ton/year) in both database (EDGAR/MEIC) and corresponding ratios for CO, NH_3, NO_x and SO_2.

Sector (MEIC)	CO	NH3	NOx	SO2
Agriculture	114566/0 NA	1303355/1910370 0.68	101858/0 NA	627/0 NA
Energy	239613/624992 0.38	928/0 NA	2419754/2747357 0.88	5810903/3142822 1.85
Industry	16603195/27933647 0.59	25155/91952 0.27	1201943/3021962 0.40	2769739/5044199 0.55
Residential	6792681/17863635 0.38	1518/87055 0.02	176073/294056 0.60	378191/1034023 0.37
Transport	1164001/6452107 0.18	3075/5802 0.53	511568/1890448 0.27	65925/56351 1.17

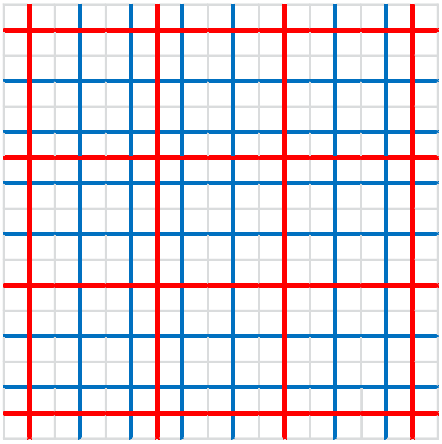

Figure 12. Correspondence between MEIC (red) and EDGAR (blue) grid cells.

The redistribution of the emissions was done using data for the same component where possible (CO, NO_x, NH_3, SO_2). For the 16 CB05 components (ALD2, ETH, OLE, TOL …) from MEIC, the data for NMVOC from EDGAR were used and for BC, OC, $PM_{2.5}$ and PM_{coarse} the data for PM_{10} were used.

2.3 HIGH RESOLUTION ISOPRENE EMISSIONS

Regarding isoprene emissions BIRA-IASB delivered input files containing top-down monthly global biogenic isoprene emissions constrained by GOME-2 formaldehyde columns that were derived with the IMAGESv2 global CTM with a resolution of 0.5° for the three summer months in 2007 and 2008 (cf. Section 1.2). For these months the MEGAN model was used to calculate hourly isoprene emissions on the model grid with a resolution of 9 km using the standard MEGAN inputs and ECMWF data for the meteorology. The grids of the global 0.5° resolution data set and 9 km resolution model grid are shown together in Figure 13.

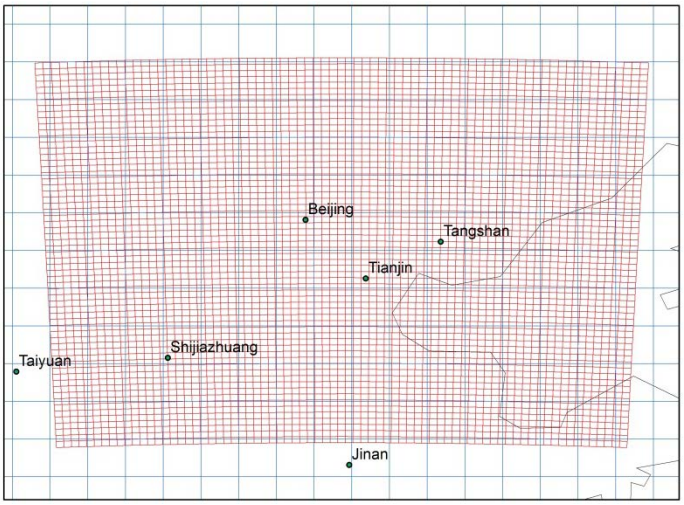

Figure 13. Model grid (red) with a 9 km resolution and 0.5° grid for the BIRA-IASB isoprene emissions.

The hourly emission results of the MEGAN run on the 9 km model grid were then aggregated to monthly values for the global grid cells of the BIRA-IASB model that were inside the model domain. The scatter plot (Figure 14) between the BIRA-IASB and the aggregated 9 km MEGAN emissions indicates that there is a good correlation between both data sets (R= 0.88) . This is not such a big surprise as also the IMAGESv2 isoprene emissions were originally derived using MEGAN. The ratio between the BIRA-IASB and free run totals were then used to calculate monthly correction factors for each 9 km grid cell and used to scale the hourly isoprene emissions on the 9 km grid.

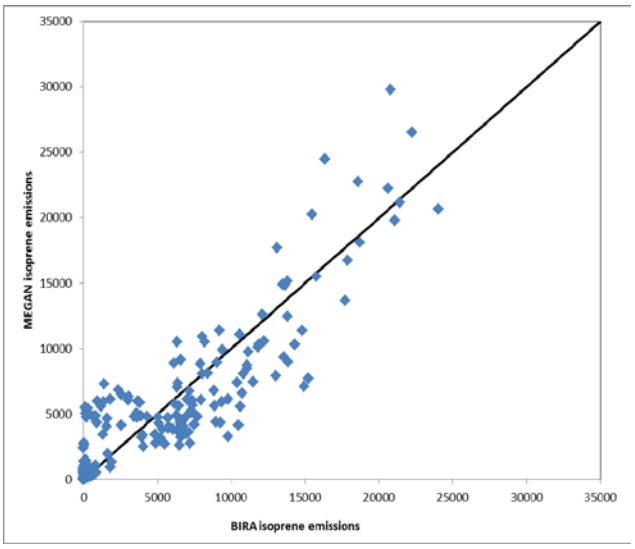

Figure 14. BIRA-IASB and MEGAN free run isoprene emissions on the 0.5° grid cells within the model domain.

As can also be seen from the scatter plot in some cases there are emissions in the MEGAN free run which are not found in the BIRA-IASB emissions (i.e. the points on the Y axis in Figure 14). In that case the scaling factor is zero and the resulting emissions will be zero. The case where there are emissions in the BIRA-IASB global data set but not in the MEGAN data set does not occur.

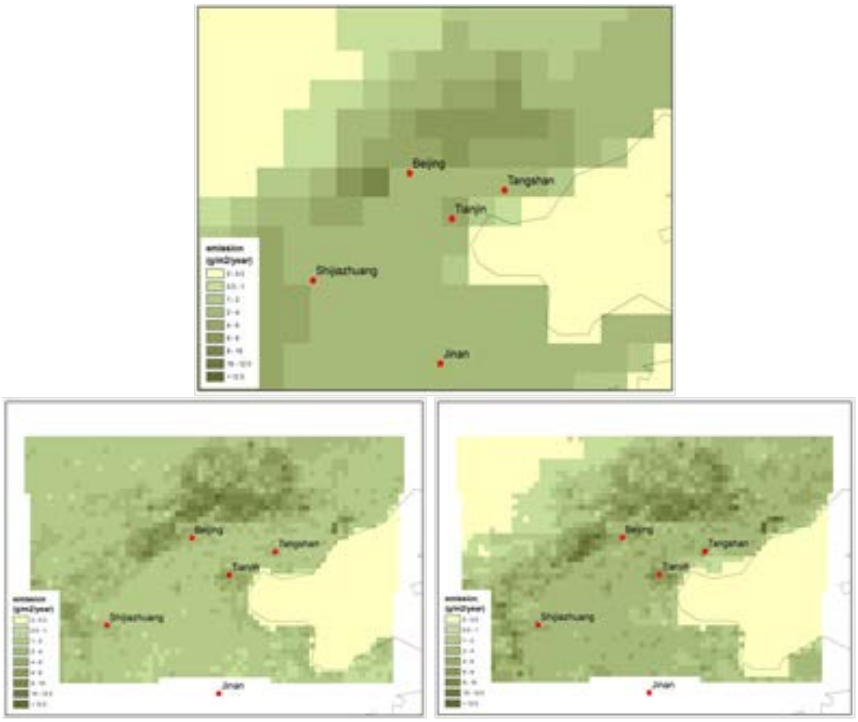

Figure 15. Isoprene emissions for August 2008 as supplied by BIRA-IASB (top) and from MEGAN at 9 km resolution before (left) and after (right) correction with the BIRA-IASB input.

2.4 HIGH RESOLUTION PYROGENIC EMISSIONS

For 2007 and 2008 BIRA-IASB supplied global data sets at 0.5° resolution for the monthly global fire emissions obtained using the IMAGESv2 global CTM constrained by GOME-2 HCHO columns. It was first attempted to use the MODIS fire products (MOD14A1 and MYD14A1) to redistribute the monthly low resolution emissions both in space and time. Some tests however revealed that there were often no fires where there were pyrogenic emissions according to the low resolution data set so that this approach would result in a significant loss of emissions as well as at times very high but short emissions. It was therefore in the end decided to spatially distribute the emissions according to a land use map obtained from the State key laboratory of Resources and Environmental Information System (REIS) in Beijing. On this map the classes referring to farm land that is not used for paddy fields (code 12) or where there is abundant grass land were considered to be potential locations where there is straw burning (Figure 16).

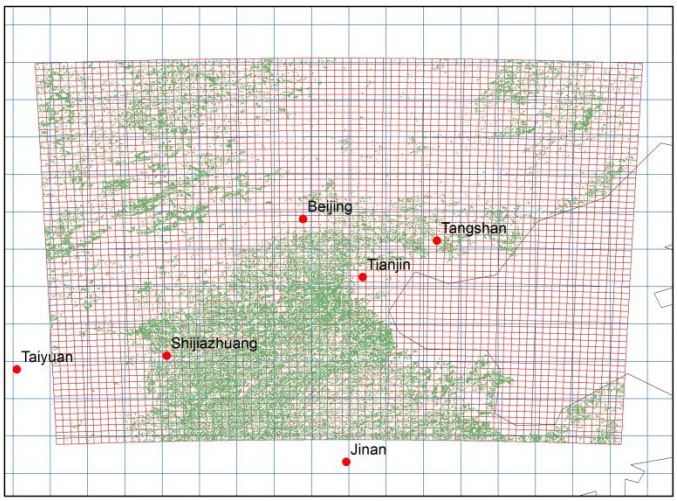

Figure 16. Land use map showing the occurrence of farmland superimposed on the global 0.5°.

The procedure to downscale the emissions consisted in assigning the 0.5° resolution pyrogenic emissions to (the parts of) the 9km resolution grid cells within the 0.5° cells to which these emissions belong according to the relative area of the cells that were occupied by 'farm land'. This was done for the different pollutants for which the pyrogenic emissions were provided by BIRA-IASB and the three summer months of 2007 and 2008. This procedure is illustrated in Figure 17.

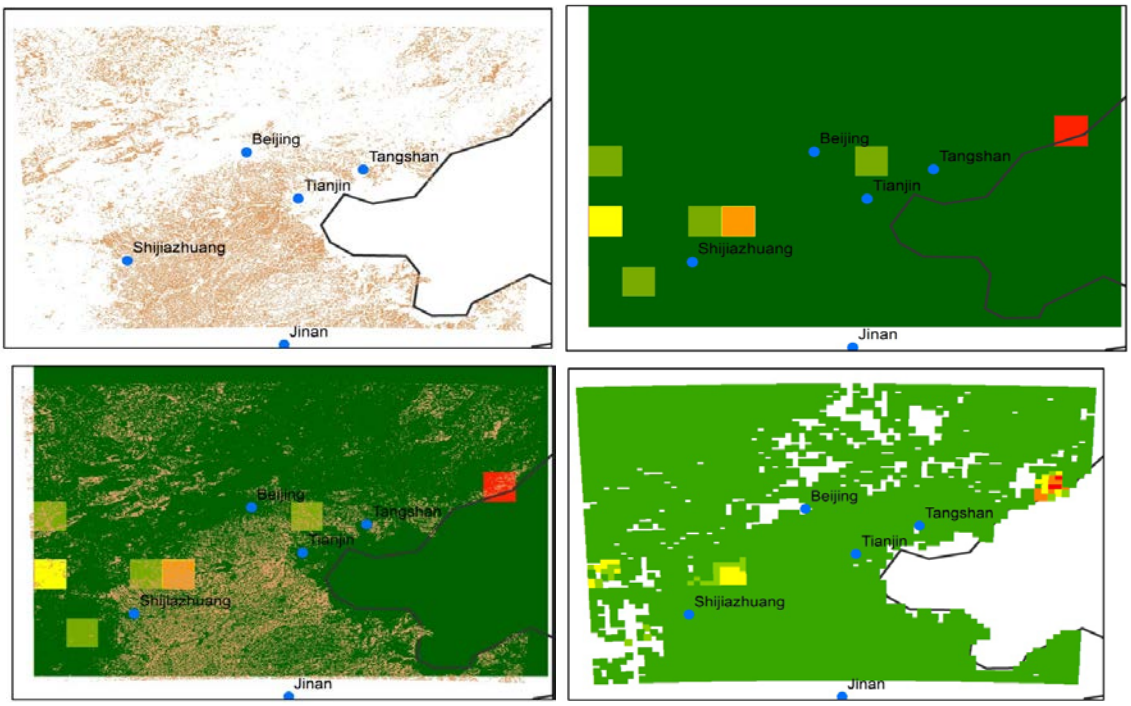

Figure 17. Downscaling of the pyrogenic methanol emissions for June 2008 (top right) using the farmland land use map (top left). The two data sets are superimposed (bottom left) and this results in 9 km resolution emission map (bottom right). The colours used for the emissions from low to high values are green (low) - yellow – orange and red (high).

3. CONTRIBUTION OF BIRA-IASB IN WP2

3.1 MAX-DOAS MEASUREMENTS OF NO_2 AND HCHO AT BEIJING AND XIANGHE

The MAX-DOAS instrument, which was designed and assembled at BIRA-IASB in Brussels, was installed during the July 2008–April 2009 period on the roof of the Institute of Atmospheric Physics (IAP) of the Chinese Academy of Sciences located in the Beijing city centre (39.98◦N, 116.38◦E). Then, it was moved to the suburban site of Xianghe (39.75◦N, 116.96◦E), located about 60 km east of Beijing where it has been operating continuously from March 2010 until now. At both locations, the azimuthal scan option was not activated and the telescope points towards a fixed azimuth direction (north). A full MAX-DOAS scan requires about ~15 min and comprises the following 9 elevation angles: 2◦, 4◦, 6◦, 8◦, 10◦, 12◦, 15◦, 30◦, and 90◦ (zenith).

The measured scattered light spectra are analysed using the spectral fitting software suite QDOAS developed at BIRA-IASB. The principle of the DOAS technique is to separate the absorption of molecular species which usually display narrow features from a broadband background resulting mainly from Mie and Rayleigh scattering and instrumental effects. The direct product of the DOAS spectral fitting method is the differential slant column density (DSCD) which is the concentration of a given absorber integrated along the effective light path relative to the amount of the same absorber in a measured reference spectrum. For profile retrieval in the troposphere, it is a common way to select the zenith measurement of a MAX-DOAS scan as the reference for the off-axis DSCDs of the same scan in order to minimise the stratospheric signal. More details on the NO_2 and HCHO datasets can be found in Vlemmix et al. (2014) and Hendrick et al. (2014).

Figure 18. The MAX-DOAS instrument at Beijing (left) and at the suburban Xianghe site (right). Location of Xianghe (bottom panel).

3.2 COMPARISONS WITH IMAGES HCHO COLUMNS

In the following figure we have compared monthly averaged MAX-DOAS HCHO columns with GOME-2 HCHO measurements obtained in a radius of 100 km around Xianghe station using either the IMAGESv2 a priori profiles in the retrieval or the locally measured MAX-DOAS profiles. As illustrated in Figure 19, the use of the MAX-DOAS profiles (when available) in the GOME-2 HCHO retrievals brings the GOME-2 HCHO columns much closer to the ground-based observations. The GOME-2 HCHO columns used in the inversion are shown in orange and are found to be by 20-30% lower than the MAX-DOAS observations, especially in summertime. The model exhibits a satisfactory agreement with the MAX-DOAS measurements during wintertime, although it is biased low, especially during fall 2011. Although the updated emissions help to reduce the discrepancy between the MAX-DOAS data and the model, the optimized columns are still by 35-40% lower than the MAX-DOAS measurements. This indicates that biogenic emissions and/or agricultural fires burning in the North China Plain remain underestimated in the model. However, the disagreement could be partly attributed to the errors caused by the

limited representativeness of point measurements when compared to columns simulated with a model at a coarse resolution.

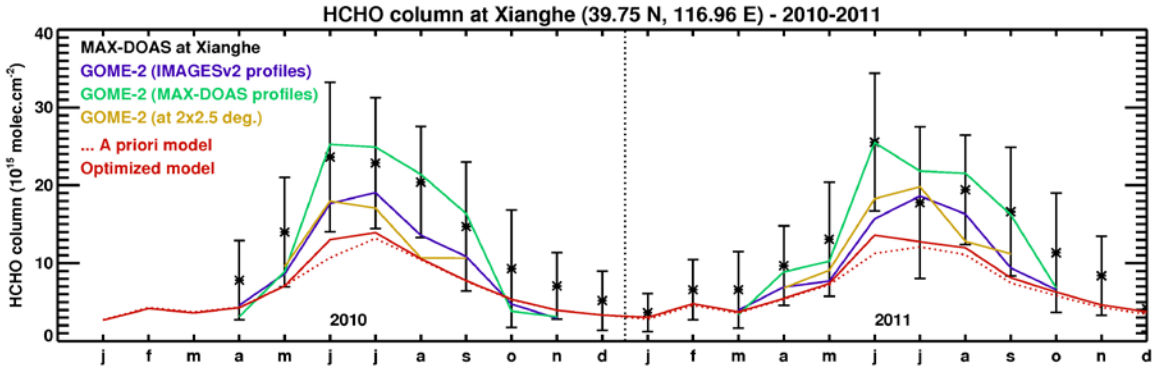

Figure 19. Comparison between monthly averaged MAX-DOAS HCHO columns (in black), GOME-2 HCHO columns using either the IMAGESv2 profiles (in blue) or the locally measured MAX-DOAS profiles (in green), the a priori model in red dotted line and the optimized model in red solid line for 2010-2011.

3.3 LATERAL CONDITIONS FROM THE IMAGESV2 MODEL

As explained earlier (Section 1.1), years 2007 and 2008 have been chosen as 'climate-change' and reference year, respectively. For those years, boundary conditions from the IMAGESV2 model have been stored in NetCdf data files and provided to VITO in order to be used as boundary and initial conditions for the high resolution AURORA model. The AURORA model has a resolution of 9 km. More specifically, 85 concentration fields have been provided in 2x2.5 degree resolution for the summer months (June, July, August) of 2007 and 2008. Additionally, top-down VOC emissions for summer 2007 and 2008 derived as explained in Section 1.3 were made available to AURORA model : top-down anthropogenic VOC emissions in 0.25x0.25 degree for summer 2007 and 2008, biogenic isoprene, as well as emissions of carbon from biomass burning in 0.5x0.5 degree. All files are available at the IBBAC web site http://tropo.aeronomie.be/ibbac/data.html

3.4 IMPACT OF BIOGENIC EMISSIONS AND METEOROLOGY

We evaluate the impact of biogenic emissions and the impact of meteorology on the concentrations of pollutants and oxidants for the 'climate change'-like year 2007 and for the reference year 2008. To this purpose, we design a sensitivity simulation for 2007 with the IMAGESv2 model where we use optimized anthropogenic and pyrogenic emissions from 2007 but isoprene emissions derived from the optimization of 2008 (S1 simulation, Table 4). To further investigate the impacts of meteorology on the modelled concentrations, we carry out an additional simulation (S2) in which the 2007 meteorology is replaced by 2008 fields. The changes in concentrations of boundary layer OH, NO, NO_2, HO_2 and O_3 are calculated between the S1 experiment and the S0 standard case (Figure 20). Further, we quantify the impact of meteorological fields by deriving the differences in concentrations between S2 and S1 (Figure 21).

Table 4. Simulations performed with IMAGESv2 to assess the impact of isoprene emissions and meteorology on pollutant concentrations.

Sensitivity simulation in 2007	Anthropogenic emissions	Biomass burning emissions	Isoprene emissions	Meteorology
S0	Optimized 2007	Optimized 2007	Optimized 2007	2007
S1	Optimized 2007	Optimized 2007	Optimized 2008	2007
S2	Optimized 2007	Optimized 2007	Optimized 2008	2008

A direct effect of isoprene emission increases, such as occurring around coastal areas in China, is a decrease in OH concentrations in the boundary layer, up to 10%, accompanied by moderate HO_2 increase.

This is mainly due to the reactions of isoprene and its oxidation products with OH, often producing HO_2. In addition, NOx concentrations are decreased in the emission regions, due to increased production of organic nitrates and peroxy acetyl nitrates (PAN), which are carried away to more remote environments, e.g. the China sea, where NOx concentrations are therefore increased (Figure 20). Of importance for air quality is the increase of surface ozone concentrations in Eastern China as a result of the increase of isoprene emission in a high NOx environment. This well-known behavior is largely explained by a competition between the ozone-producing HO_2+NO reaction (followed by a photolysis of the formed NO_2) and the ozone-destroying HO_2+O_3 reaction. The ozone increase is estimated at up to 3% in megacities (Table 5).

The differences seen on Figure 21 are due to meteorology alone. These changes are found to be often more important than the isoprene-associated changes, especially over the oceans, where they are mostly driven by changes in circulation between 2007 and 2008. The decrease by 15% of the ozone concentration in Central China is due to the cooler conditions prevailing in 2008 (as seen from the lower isoprene emissions in 2008, Figure 20). The opposite pattern is seen in North-central India where the positive change in ozone (around 10%) can be attributed to warmer weather conditions in 2008 in this region. In Beijing and Shanghai, the changes due to meteorology are similar to those associated with isoprene emission changes.

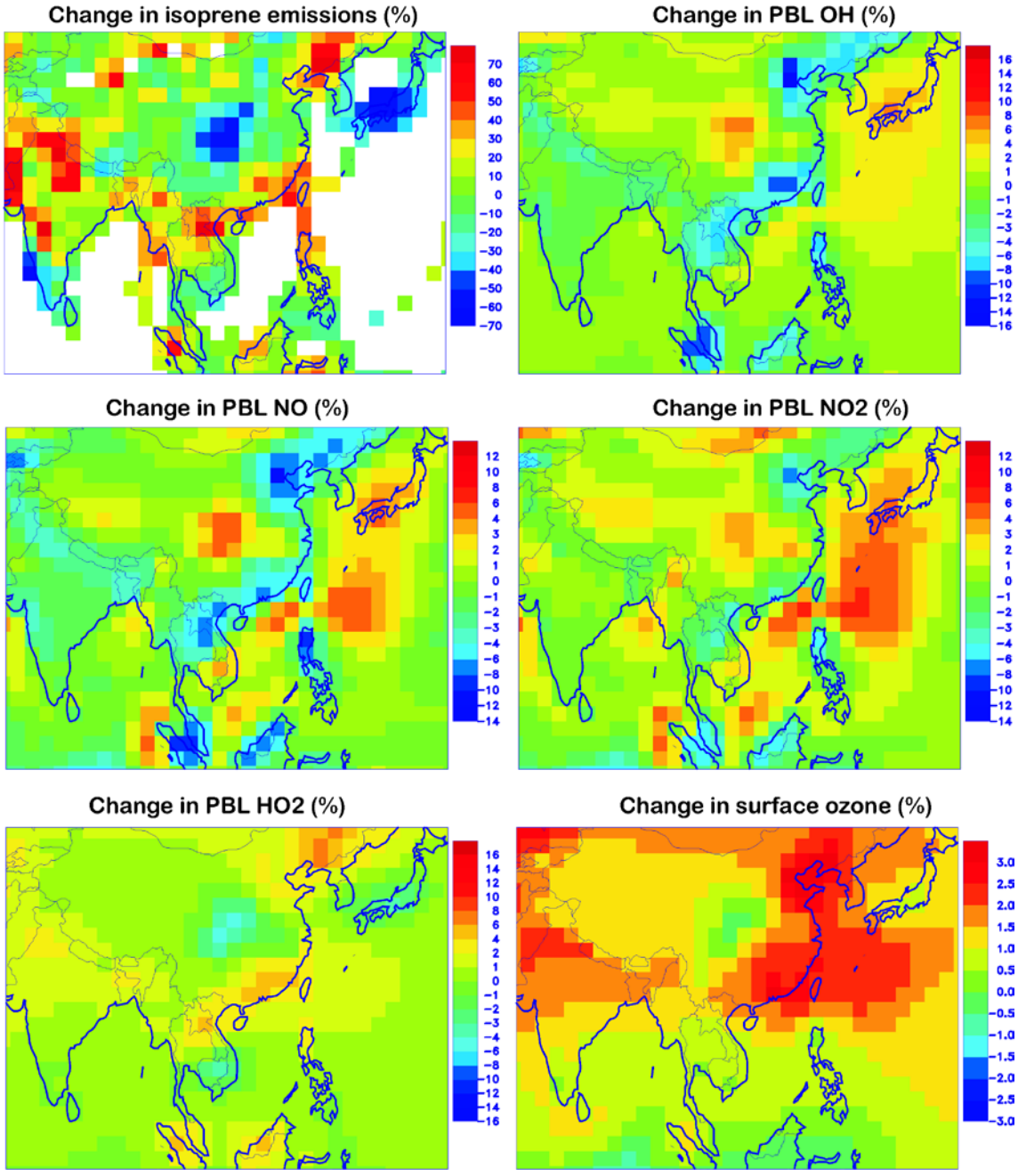

Figure 20. Calculated changes in isoprene emissions, boundary layer OH, NO, NO_2, HO_2, and surface ozone between S1 and S0, ((S1-S0)/S0)x100, in July 2007.

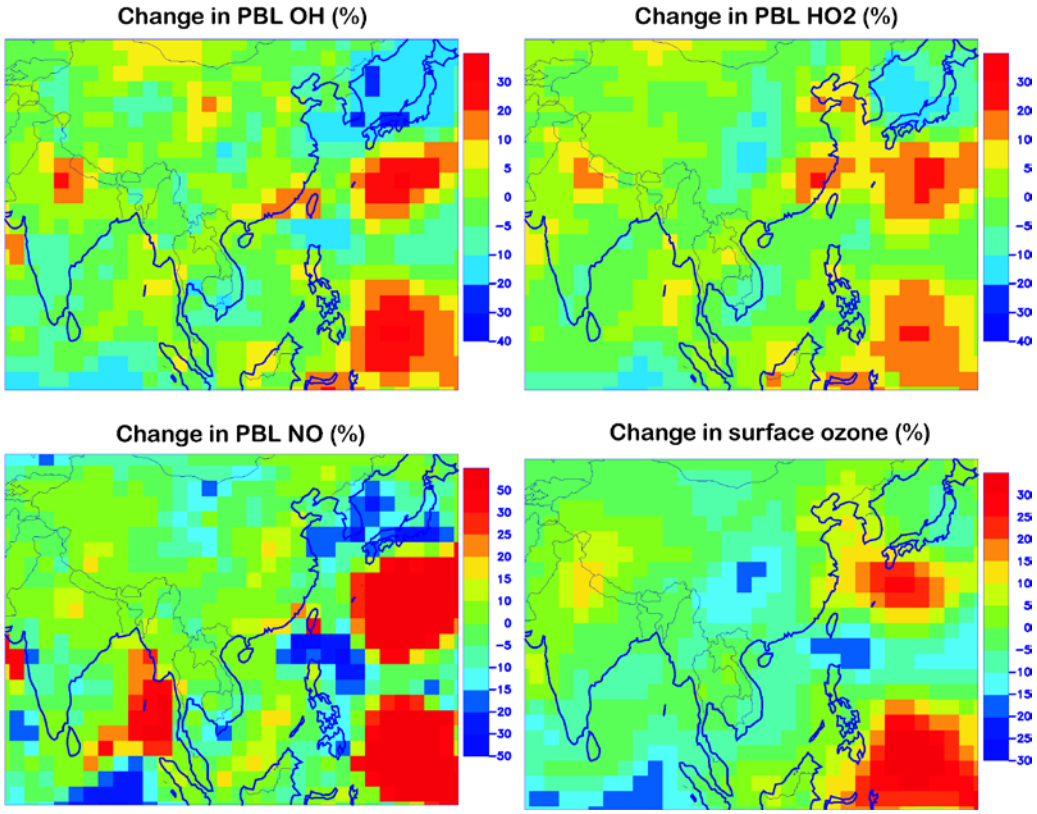

Figure 21. Calculated changes in boundary layer OH, NO, and surface ozone between S2 and S1 simulations, ((S2-S1)/S1)x100, in July 2007. Isoprene emissions are kept constant in these simulations and equal to their 2008 value.

Table 5. Changes in surface ozone at Chinese megacities calculated with IMAGESv2 (i) due to isoprene emissions (ii) due to meteorology.

Change in surface ozone at	Due to isoprene emissions	Due to meteorology
Beijing	3.1%	3.3%
Shanghai	2.2%	6.8%
Hong Kong	3.4%	-6.3%
Chengdu-Chongqing	0%	-16%

4. CONTRIBUTION OF VITO IN WP2

4.1 HIGH RESOLUTION CONCENTRATION MAPS FOR BEIJING - INTRODUCTION

In work package 2 the aim is to set up a high resolution model with AURORA for an area covering Beijing in which we use the high resolution emission data sets prepared in work package 1. The results of the model should then be validated and compared to the results of the IMAGESv2 model. The intention is to set up a model for a reference year as well as for a climate change scenario so that the effects of increases in biogenic isoprene emissions can be investigated. For the reference year 2008 was selected while for the climate change scenario the meteorology of the year 2007 was used. For these two years BIRA-IASB delivered daily average concentration results from the IMAGESv2 model at the resolution of 2x2.5 degrees for the summer months (June, July and August) of 2007 and 2008. These low resolution concentrations were used as boundary and initial conditions input in the AURORA model. The AURORA model itself was set up with a resolution of 9 km. For the meteorological input data ECMWF forecast results at a resolution of 0.125° were used.

4.2 VALIDATION AND COMPARISON OF MODEL RESULTS

For 2008 we received the following measurement data sets from BIRA-IASB:

- HCHO total columns [molec./cm^2] and surface concentration [molec./cm^3] for lowest 100 m measured using MAXDOAS from the roof of the IAP building (116°22 East, 39°58 North) for 3/7/2008 – 17/4/2009 by Tim Vlemmix (BIRA-IASB).
- NO_2 total columns [molec./cm^2] and surface concentrations [molec./cm^3] for lowest 200 m measured using MAXDOAS from the roof of the IAP building (116°22 East, 39°58 North) for 22/6/2008 – 30/9/2008 by François Hendrick (BIRA-IASB).
- surface NO_2 concentrations [ppb] for 1/7/2008 – 20/9/2008 measured at three different heights (8m, 120 m and 280 m) on a tower nearby IAP that were provided by IAP, via Yu Huan. (ref: Xin J. Y., Wang Y. S., Tang G. Q., et al.: Variability and reduction of atmospheric pollutants in Beijing and its surrounding area during the Beijing 2008 Olympic Games, Chinese Sci. Bull., 2010, 55: 1937-1944, doi: 10.1007/s1434-010-3216-2).

In Figure 22 the average daily total column HCHO observed using MAX-DOAS is compared to the values calculated by AURORA and IMAGESv2. At first sight the AURORA results seem to be in better agreement. The correlation of the IMAGESv2 (0.41) results is however better than for AURORA (0.22) where maxima and minima don't always coincide well between model results and observations. Both models underestimate the observed values but the average bias is slightly better for AURORA that underestimates the observations by 47% on average compared to 54 % for IMAGESv2.

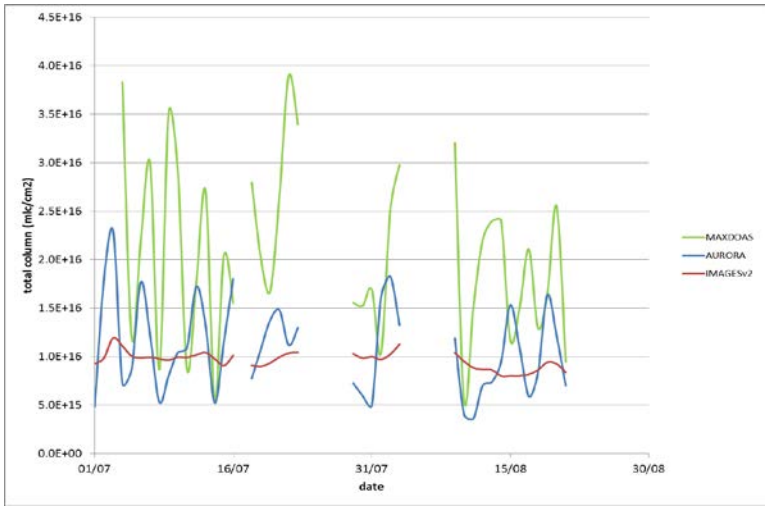

Figure 22. Daily average total column HCHO (molec./cm^2) from the MAXDOAS observations and the IMAGESv2 and AURORA models.

For NO_2 the modelled concentrations are of the same magnitude as the MAX-DOAS measurements (Figure 23). On average AURORA overestimates the MAX-DOAS measurements by 7% while IMAGESv2 underestimates these measurements by 78% i.e. the observations are on average 5 times larger than the IMAGESv2 results. From Figure 23 it is also clear that the variance of the AURORA results (9.E+22 molec.^{2}/cm^6) is in better agreement with the variance of the measurements (6.E+22 molec.^{2}/cm^6) than this is the case for the IMAGESv2 (1.E+20 molec.^{2}/cm^6) results. A possible explanation for this difference between the IMAGESv2 results and the measurements could be the more local character of a pollutant such as NO_2. In this sense the IMAGESv2 results are more representative for the background concentration than the AURORA results. This difference in spatial detail is also obvious from Figure 24.

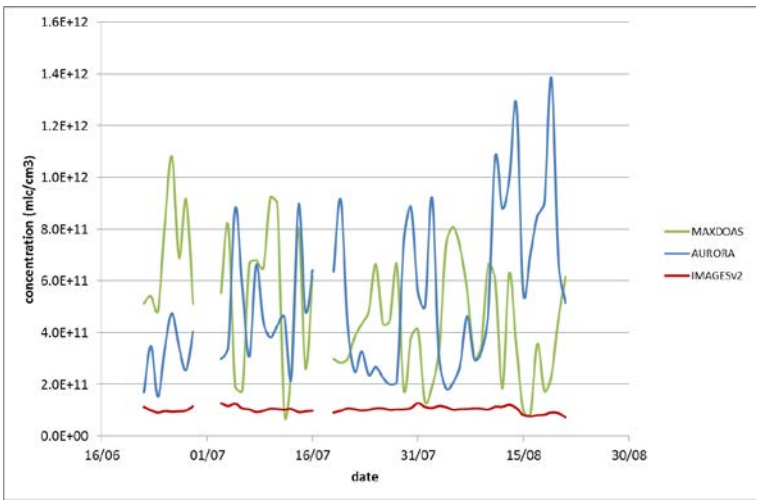

Figure 23. Daily average near surface (<200m) NO_2 concentration (molec./cm^3) from the MAXDOAS observations and the IMAGESv2 and AURORA models.

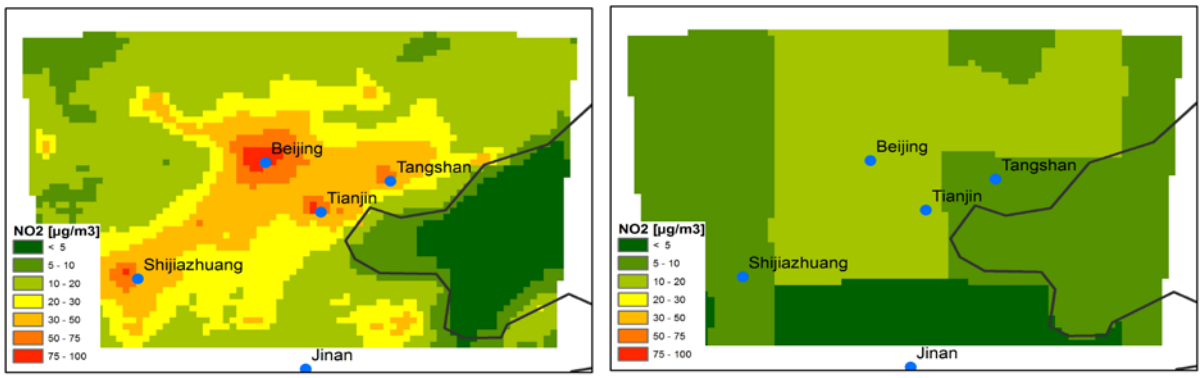

Figure 24. Average NO_2 concentration (µg/m^3) based on the AURORA and the IMAGESv2 concentrations for June – August, 2008.

These same conclusions can also be drawn from the comparison with the Xin et al. (2010) NO_2 measurements (Figure 25). Also here the AURORA modelled concentrations are in better agreement with the measurements both in terms of the average magnitude and the temporal variation. A possible explanation for the overestimation of the measured concentrations by AURORA in August is that the model does not explicitly take into account the pollution abatement measures that were taken during the Summer Olympics which took place in Beijing from 8 to 24 August, 2008. Finally, we compare the MAX-DOAS measurements to the measurements at 120 m height (Figure 26). Based on the hourly values, the correlation between the measurement time series amounts to 0.61 while the concentration measured at 120 m height on the tower is 37% lower than the MAX-DOAS measurement. When the comparison is based on the daily average values the bias is reduced to a mere 3% and correlation increases to 0.66.

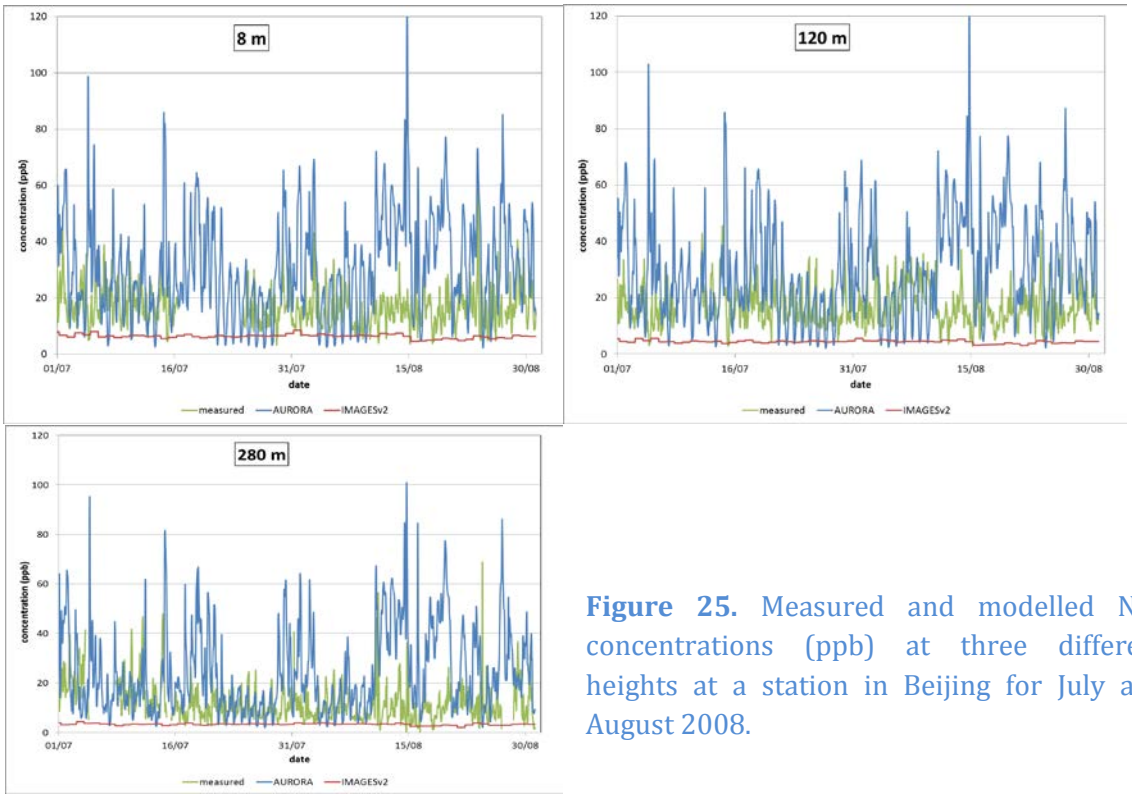

Figure 25. Measured and modelled NO_2 concentrations (ppb) at three different heights at a station in Beijing for July and August 2008.

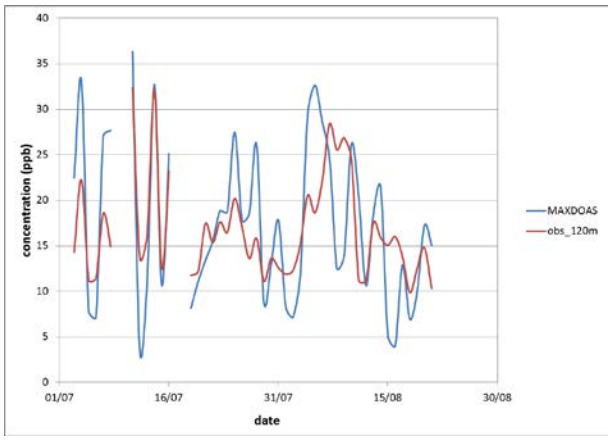

Figure 26. Daily average concentration based on the MAX-DOAS measurements and the measurements from a tower nearby at 120m height. MAX-DOAS measurements were converted from molec./cm^3 to ppb assuming a surface pressure of 1013.25 hPa and a temperature of 25 °C.

4.3 MODEL RESULTS FOR THE REFERENCE YEAR

The year 2008 for which measurements were available was also selected as the reference year. As boundary and initial conditions for the concentration calculation the daily average concentration results from the IMAGESv2 model at the resolution of 2x2.5 degrees for the summer months (June, July and August) 2008 were used. The AURORA model itself was set up with a resolution of 9 km. For the meteorological input data ECMWF forecast results for the summer of 2008 at a resolution of 0.125° were used. AURORA average concentrations for the pollutants $PM_{2.5}$, PM_{10}, O_3, and NO_2 during the summer months of 2008 are shown in Figure 27.

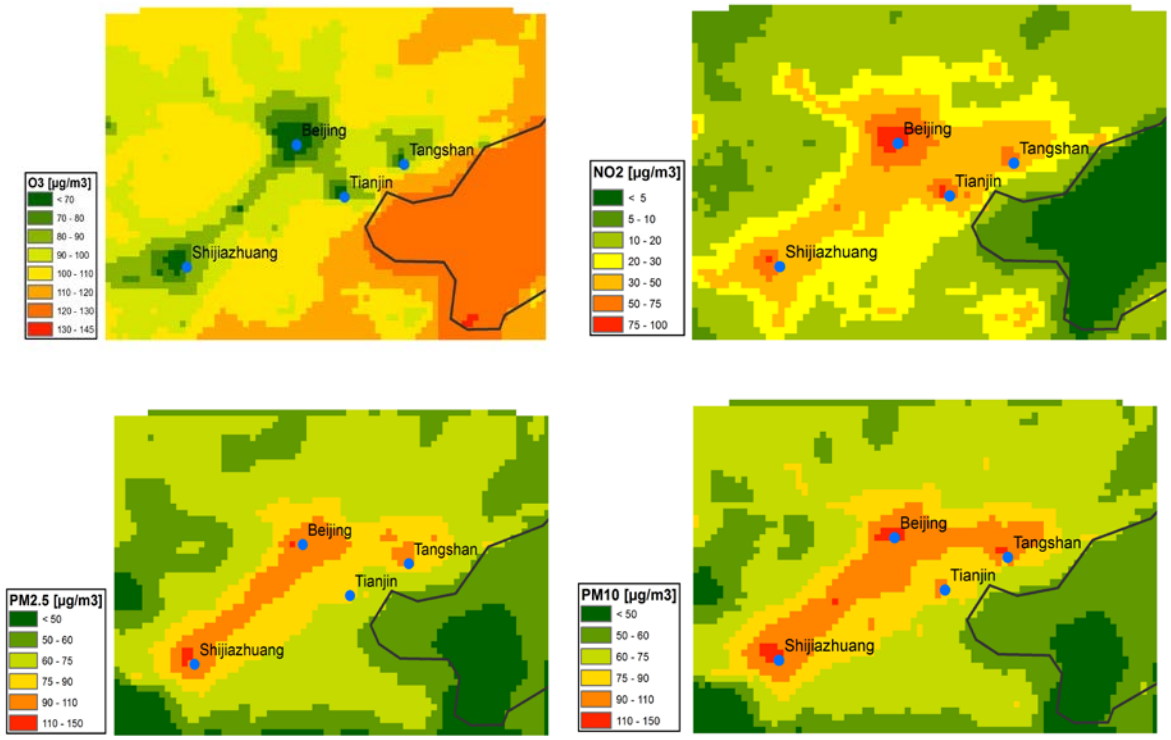

Figure 27. Average O_3,NO_2, $PM_{2.5}$ and PM_{10} concentrations (µg/m^3) in the model area for the months June- August 2008.

As can be seen in the figures, densely populated areas such as Beijing are characterized by relatively higher NO_2 and PM levels while O_3 levels are lower than in the surrounding areas where NO_2 concentrations are lower.

Table 6. Average composition of the particulate matter (PM) in the model area and in Beijing. OC: Organic carbon, EC: Elementary carbon, SOA: secondary organic aerosol, PIA: primary inorganic aerosol, NH_4: ammonium, NIT: nitrate, SO_4: sulphate, IA: inorganic aerosol, OA: organic aerosol.

Size bin (µm)	Fraction	Concentration (µg/m³)	
		Whole domain	Beijing
0 – 2.5	OC	10.68	11.78
	EC	1.96	3.81
	SOA	2.08	2.49
	PIA	6.99	15.59
	NH4	10.55	15.29
	NIT	7.12	15.86
	SO4	24.58	28.63
	Total	**63.94**	**93.45**
2.5 - 10	IA	1.76	4.57
	OA	0.44	1.13
	Total	**2.20**	**5.70**

The composition of the particulate matter (PM) for both the entire model area as Beijing is given in Table 6. From this table it can be seen that most of the PM is in the fine fraction. For the model domain the coarse (2.5 -10 µm) fraction is at most 12% of the total PM_{10} with an average of 3%. In Beijing the coarse fraction is 6% of total PM_{10} mass. According to the model most of the fine fraction consists of secondary inorganic aerosol that is ammonium (NH_4), nitrate (NIT) and sulphate (SO_4): 66% of total $PM_{2.5}$ mass on average and 64 % in Beijing. Noticeable is the larger contribution of nitrate (NIT) and the primary inorganic aerosol in Beijing compared to the average for the whole domain. Overall the organic aerosol fraction calculated by AURORA seems to be rather (too) small. The organic carbon (OC) fraction in the calculation contains all non-elementary carbon (EC) boundary condition contributions as well as a fraction of the coarse PM emissions. For the fine fraction PM emissions it is assumed that these are only inorganic. The fraction designated as 'SOA' is in this case the fraction that is generated within the model domain by AURORA by oxidation of VOCs and does not take into account the secondary organic aerosol contributions from the boundary conditions. The total secondary organic aerosol contribution is therefore this SOA fraction and a fraction of the organic carbon (OC) contribution from the boundary and initial conditions. As the PM_{10} distribution is very similar to the $PM_{2.5}$ and the coarse fraction is less prominent, the discussion in the rest of the text will be limited to the $PM_{2.5}$ fraction.

4.4 MODEL RESULTS FOR THE CLIMATE CHANGE SCENARIO

For the climate change scenario the model was rerun for the summer of 2007. The input data for this run differs from the 2008 reference run in the meteorological input, the boundary and initial conditions and some of the emission inputs. The meteorological input for the scenario run is based on the ECMWF forecast results for July – August 2007. For the boundary and initial conditions the IMAGESv2 results for the summer of 2007 were used. The emission inputs for the biogenic, the pyrogenic and the anthropogenic VOC emissions are the summer 2007 data that were derived as described in Section 2 of this document. For NO_x, SO_x, NH_3, CO, black carbon (BC), organic carbon (OC), $PM_{2.5}$ and PM_{coarse} the same emission were used as in the reference run. Only the temporal disaggregation in 2007 and 2008 for these emissions is somewhat different due to a different number of working and weekend days for these month in 2007 and 2008 but these are minor differences (e.g. 0.7% for the NO_2 emission).

The average concentration results for the main pollutants are shown in Figure 28. The differences in concentration with the reference for these pollutants can be seen in Figure 29.

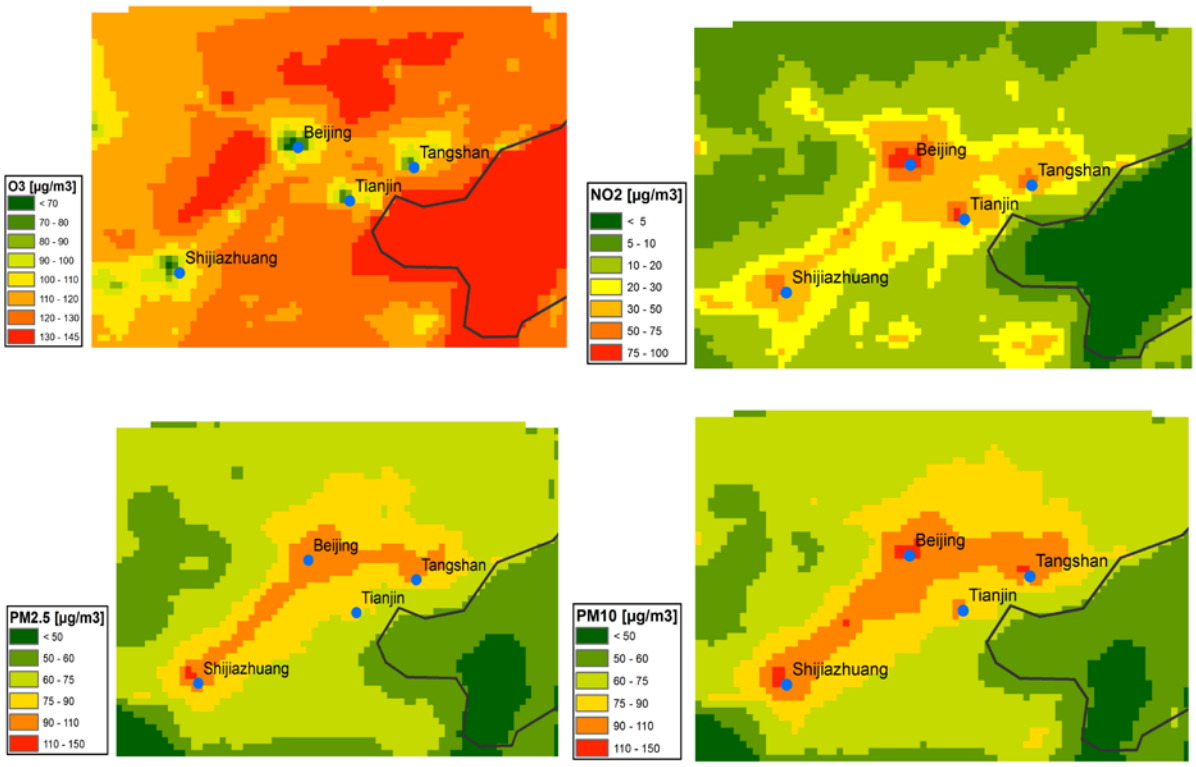

Figure 28. Average O_3, NO_2, $PM_{2.5}$ and PM_{10} concentrations (µg/m³) in the model area for the months June, July and August 2008.

For O_3 on average the concentration increases with 17 µg/m³ with a minimum increase of almost 5 µg/m³ and a maximum of 38 µg/m³. According to the model the highest increases will be in the area between Beijing and Shijiazhuang which is even in the reference case (Figure 27) an area that is characterized with higher concentrations not only for O_3 but also NO_2 and PM. Somewhat surprising are the lower NO_2 concentrations that are seen compared to the reference run. On average the NO_2 concentration decreases by 3 µg/m³ and only in Beijing we see an

increase of almost 3 µg/m^3. For PM we see an increase over the area Northeast of Beijing and along the model area boundaries which can be in excess of 5 µg/m^3. However, in the heavily polluted area between Beijing and Shijiazhuang concentrations decrease. The composition of the PM is again dominated by the inorganic fine (< 2.5 µm) fraction but there is a shift from nitrate to sulphate (Table 7).

Table 7. Average composition of the particulate matter (PM) in the model area and in Beijing (cf. Table 6).

Size bin (µm)	Fraction	Concentration (µg/m^3)	
		Whole domain	Beijing
0 – 2.5	OC	11.41 (+0.73)	12.14 (+0.36)
	EC	1.98 (+0.02)	3.58 (-0.23)
	SOA	2.30 (+0.22)	3.27 (+0.78)
	PIA	6.56 (-0.43)	14.20 (-1.38)
	NH4	10.96 (+0.41)	15.42 (+0.13)
	NIT	5.63 (-1.49)	12.07 (-3.79)
	SO4	27.07 (+2.49)	32.14 (+3.51)
	Total	**65.91 (+1.95)**	**92.82 (-0.63)**
2.5 - 10	IA	1.75 (-0.01)	4.51 (-0.06)
	OA	0.43 (-0.01)	1.11 (-0.02)
	Total	**2.19 (-0.01)**	**5.62 (-0.09)**

To further investigate the effect of the different elements that contribute to the differences between the scenario and the reference run the following runs were conducted :

1) 2007 with emissions, meteorology and boundary conditions for 2007 i.e. the actual scenario;

2) Same as 1) but with meteorology and emissions 2008: effect of boundary conditions;

3) Same as 1) but with boundary conditions and emissions 2008: effect of meteorology;

4) Same as 1) but with boundary condition and meteorology 2008: effect of the emissions.

Stated differently the runs 2) – 4) correspond to runs with the inputs of the reference (2008) run in which respectively boundary conditions, the meteorology and the emissions are replaced with the inputs for the scenario run.

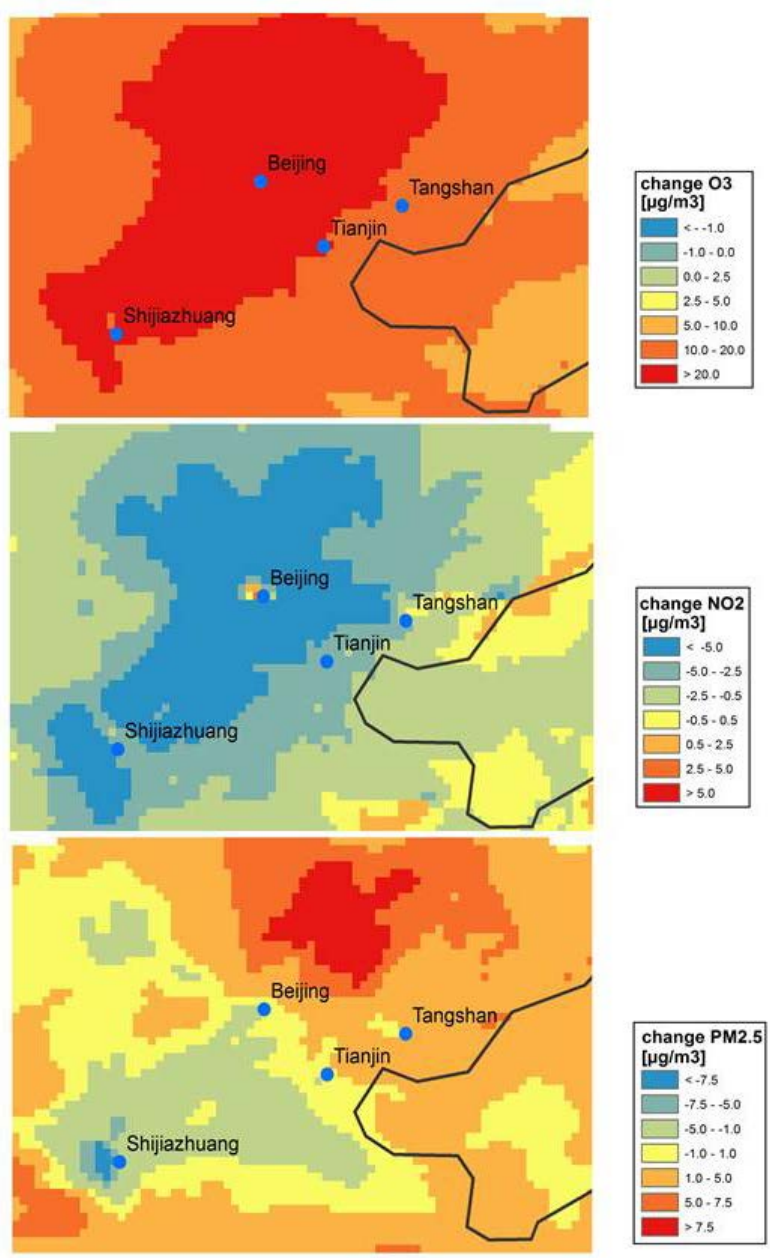

Figure 29. Changes in average concentration for the summer months between the reference (2008) and the scenario (2007) run.

For O_3 the concentration changes due to the scenario and due to the changes in boundary condition, meteorology and emissions are shown in Figure 30. In the case of O_3, the change in boundary conditions results in an increase of the average O_3 concentration over most of the model domain with between 5 and 10 µg/m^3. The emissions result in an increase of concentration over the whole domain but mainly in an area covering Beijing large increases are seen which can be in excess of 20 µg/m^3. As can be seen from this figure, the meteorology alone can't explain the increases that are seen for the O_3 concentration in the scenario run : in the southeastern part of the domain the meteorology alone even results in a decrease of the O_3 concentrations.

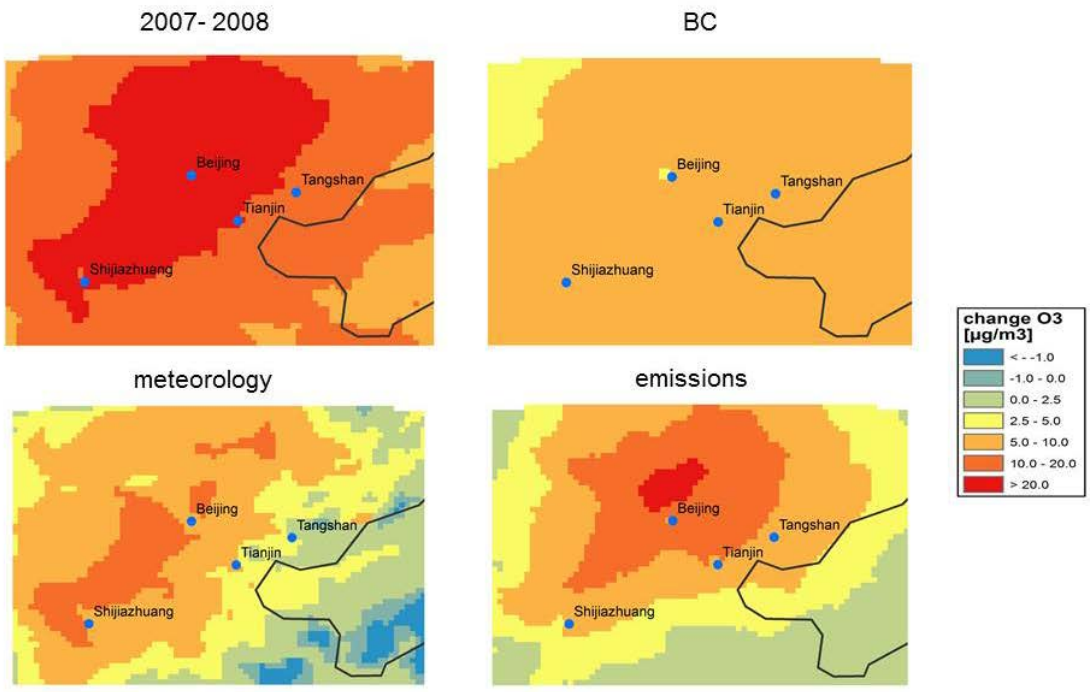

Figure 30. Change in average concentration [µg/m^3] during the summer for O_3 between the reference (2008) and the scenario (2007) calculation as well as the effect of only changing the boundary condition (BC, upper right), meteorology (lower left) and emissions (lower right).

As all non-VOC emissions are the same in the reference run and the scenario run if we neglect the slight differences due to the time distribution factor and the small contribution of biogenic NO (only 1% of the total NO emission). The change in O_3 due to the emissions alone should therefore be due to changes in the VOC emissions (Figure 18). For the scenario run mainly the anthropogenic emissions have increased and these increases are mainly in an area confined by Beijing, Tianjin and Shijiazhuang. As can be seen from the figure with the differences these are determined by the low resolution IMAGES v2 modelling results and there is a somewhat artificial, sudden change when moving south of Shijiazhuang. The fact that there was more sunlight in 2007 (293 W/m^2) than in 2008 (267 W/m^2) can help explain the higher O_3 concentrations due to the change in meteorology.

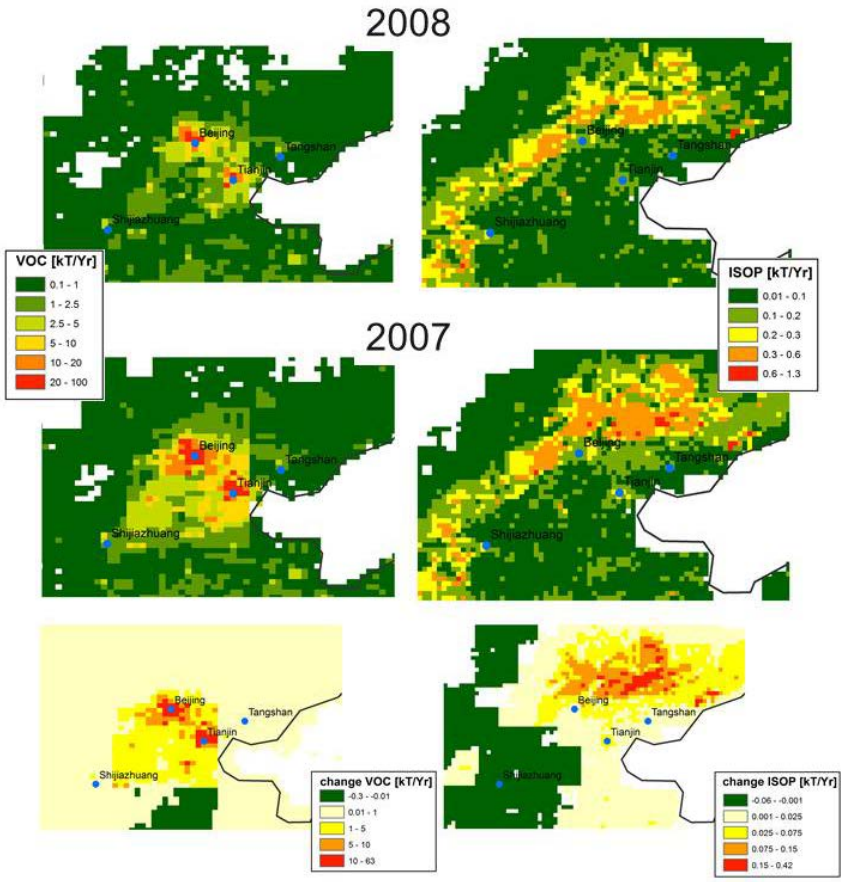

Figure 31. Anthropogenic VOC (left) and isoprene (ISOP) emission for 2007 and 2008 and difference between these emissions (notice that the scales are different!)

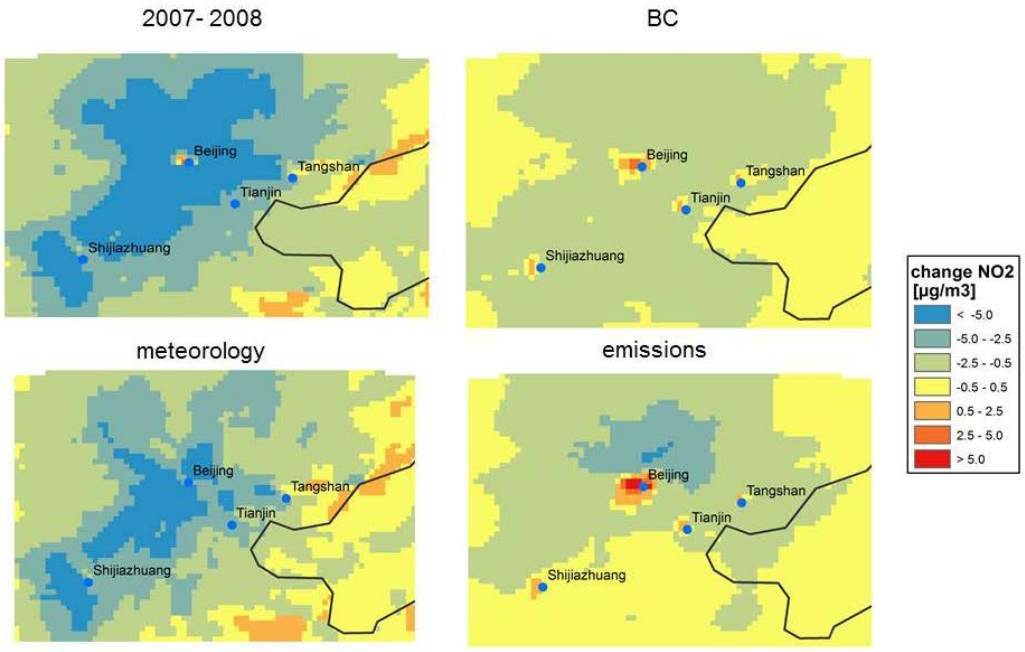

Figure 32. Change in average concentration [µg/m^3] during the summer for NO_2 between the reference (2008) and the scenario (2007) calculation as well as the effect of only changing the boundary condition (BC, upper right), meteorology (lower left) and emissions (lower right) between the scenario and the reference run.

For NO_2 the reason for the decrease in concentrations was further explored. If we consider not only NO_2 but also other gaseous components such as NO, HNO_3 (nitric acid) and PAN (peroxyacetyl nitrate and similar pollutants) we see a clear shift from less (NO, NO_2) to more oxidized forms of gaseous nitrogen (HNO_3 and PAN) (Figure 33). As the NOx emissions hardly change from the reference to the scenario and this seems to be related to the higher O_3 concentration but also to the increases in VOC emissions. The latter is reflected in the increase in PAN concentrations due to emission changes (lower right of Figure 34). The lower NO (Figure 35) and to a lesser extent NO_2 (Figure 32) concentrations are apparently linked to the changes in meteorology. The wind speed in 2007 (7.00 m/s) was on average 0.22 m/s higher 2008 (6.78 m/s) and also PBLH in 2007 (677 m) was on average 13% higher than in 2008 (597 m). These two factors can explain a general decrease in concentration. The higher O_3 concentrations due to the change in meteorology (Figure 30) can also explain the shift from NO and NO_2 to HNO_3. For NO and NO_2 the effect of the change in boundary condition is not at the boundaries themselves but mainly inside the model domain indicating that also in this case the indirect effect of a conversion to mainly HNO_3 near the polluted areas and PAN further away from the cities explains the lower NO and NO_2 concentrations.

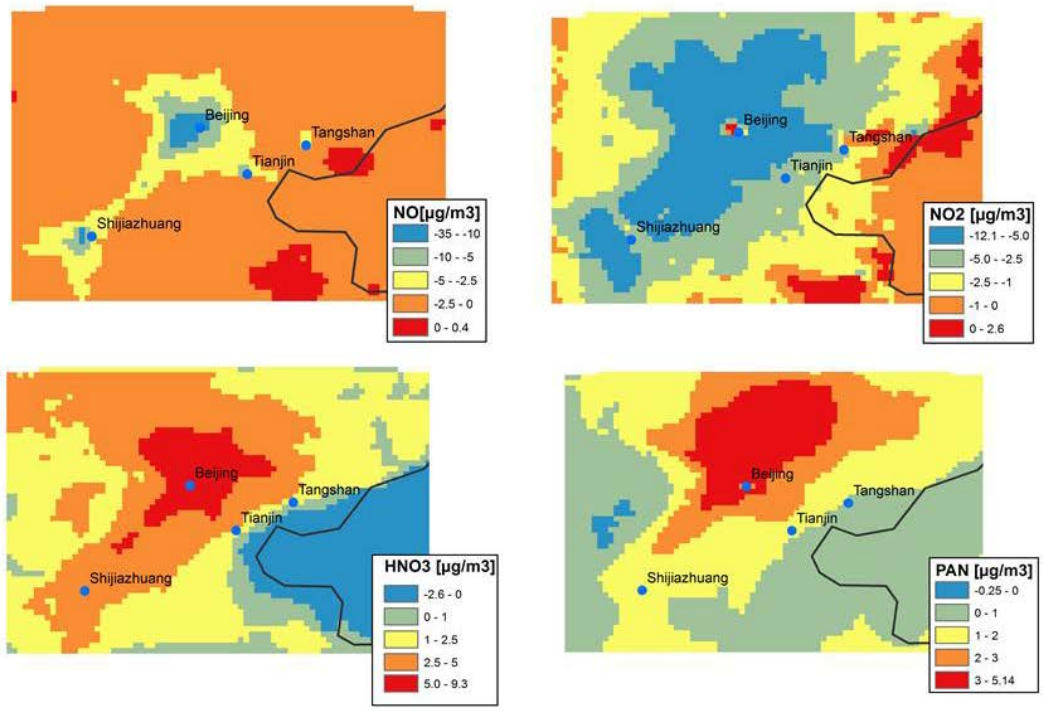

Figure 33. Change in different gaseous nitrogen species between the reference and the scenario run: nitrogen monoxide(NO), nitrogen dioxide (NO_2), nitric acid (HNO_3) and peroxyacetyl nitrate and analogues (PAN).

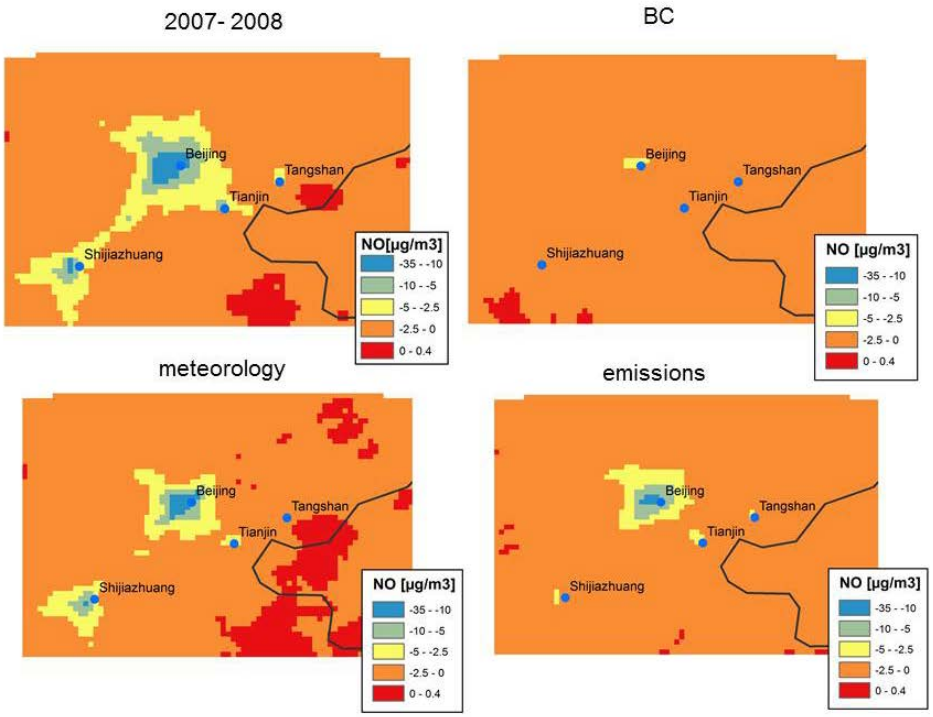

Figure 34. Change average concentration [µg/m^3] during the summer for NO between the reference (2008) and the scenario (2007) calculation as well as the effect of only changing the boundary condition (BC, upper right), meteorology (lower left) and emissions (lower right) between the scenario and the reference run.

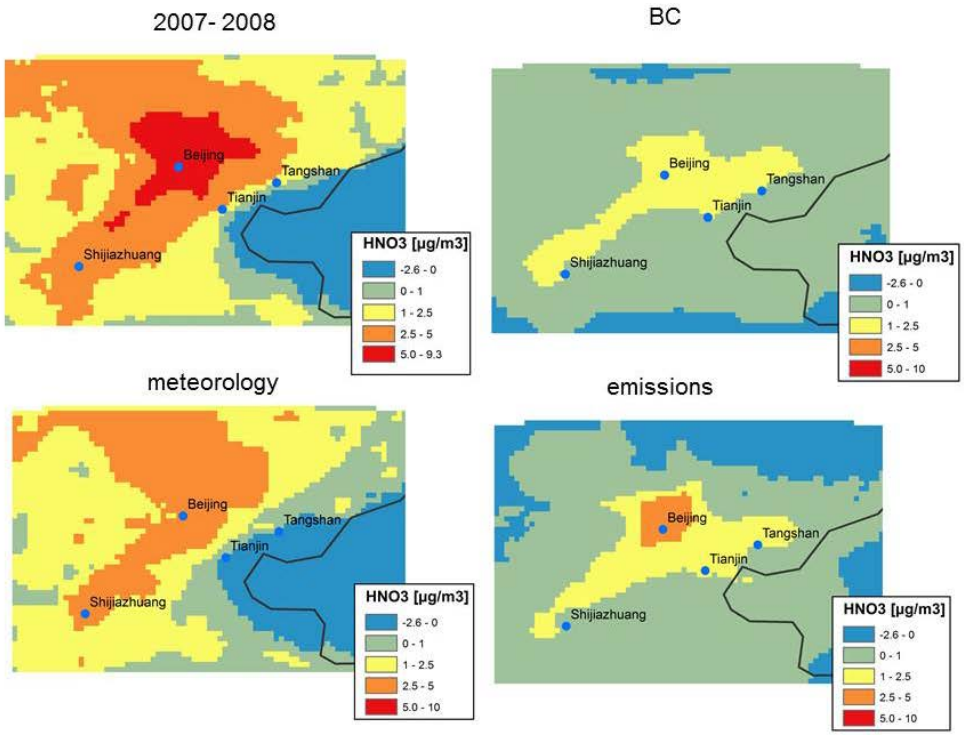

Figure 35. Change in average concentration [µg/m^3] during the summer for HNO_3 between the reference (2008) and the scenario (2007) calculation as well as the effect of only changing the

boundary condition (BC, upper right), meteorology (lower left) and emissions (lower right) between the scenario and the reference run.

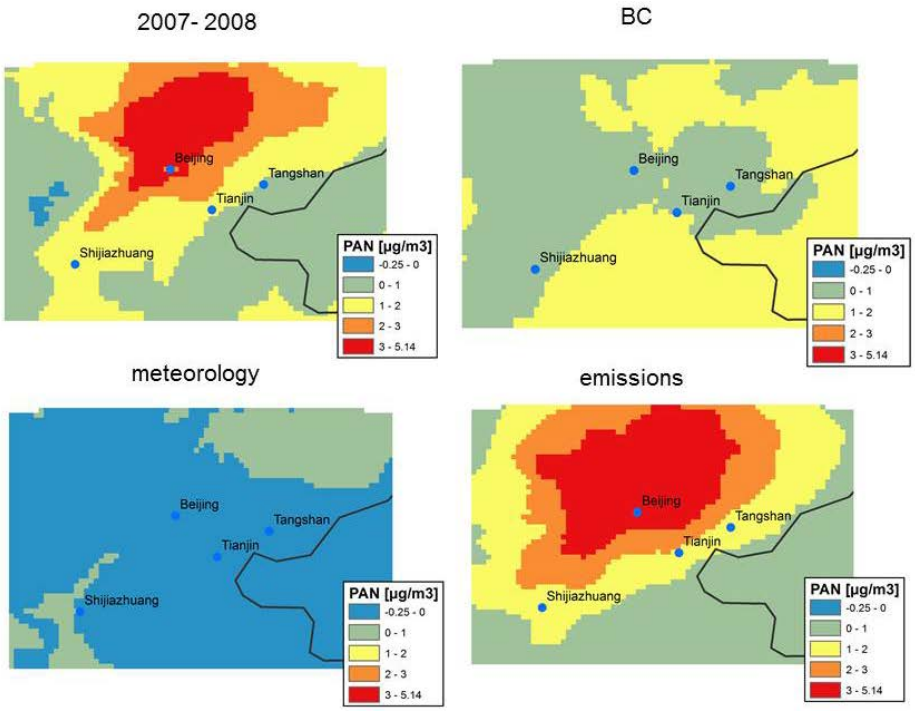

Figure 36. Change in average concentration [µg/m³] during the summer for PAN between the reference (2008) and the scenario (2007) calculation as well as the effect of only changing the boundary condition (BC, upper right), meteorology (lower left) and emissions (lower right) between the scenario and the reference run.

The changes in PM concentrations are also not related directly to emission changes except for the small change in SOA concentration (on average + 0.78 µg/m³) which can be linked to the change in VOC concentrations. The change in PM2.5 concentration can mainly be attributed to the change in the boundary condition and the meteorology where the first results in an increase while the latter tends to decrease the concentration. The decrease due to the meteorology can again be linked to the higher wind speed and boundary layer height. The main contribution to the fine PM fraction is according to the model the secondary inorganic aerosol (SIA) fraction (Table 3 and Table 4). In the scenario run there is due to higher sulphuric acid concentrations also more sulphate formation which results in lower nitrate formation as the available ammonium preferentially reacts to form ammonium sulphate. This can also be seen in the concentration change for the individual SIA components (Figure 25). Over the whole model domain an increase in sulphate is calculated while only in places with smaller sulphate concentration increases an increase in nitrate concentration is calculated.

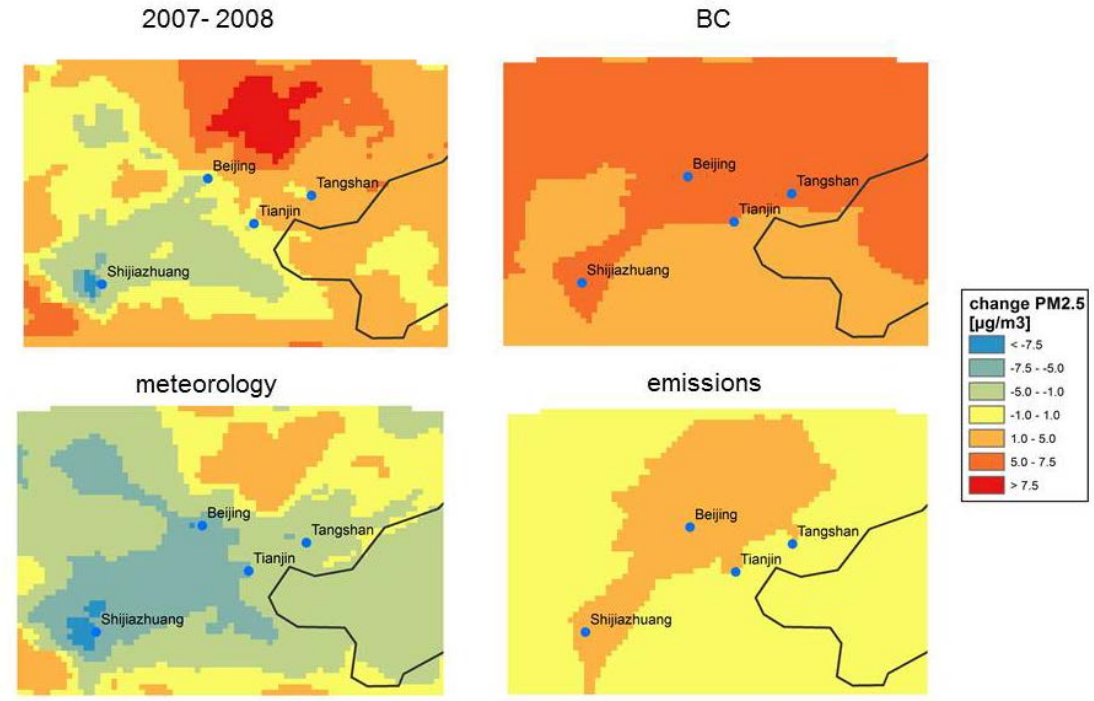

Figure 37. Change in average concentration [µg/m^3] during the summer for $PM_{2.5}$ between the reference (2008) and the scenario (2007) calculation as well as the effect of only changing the boundary condition (BC, upper right), meteorology (lower left) and emissions (lower right) between the scenario and the reference run.

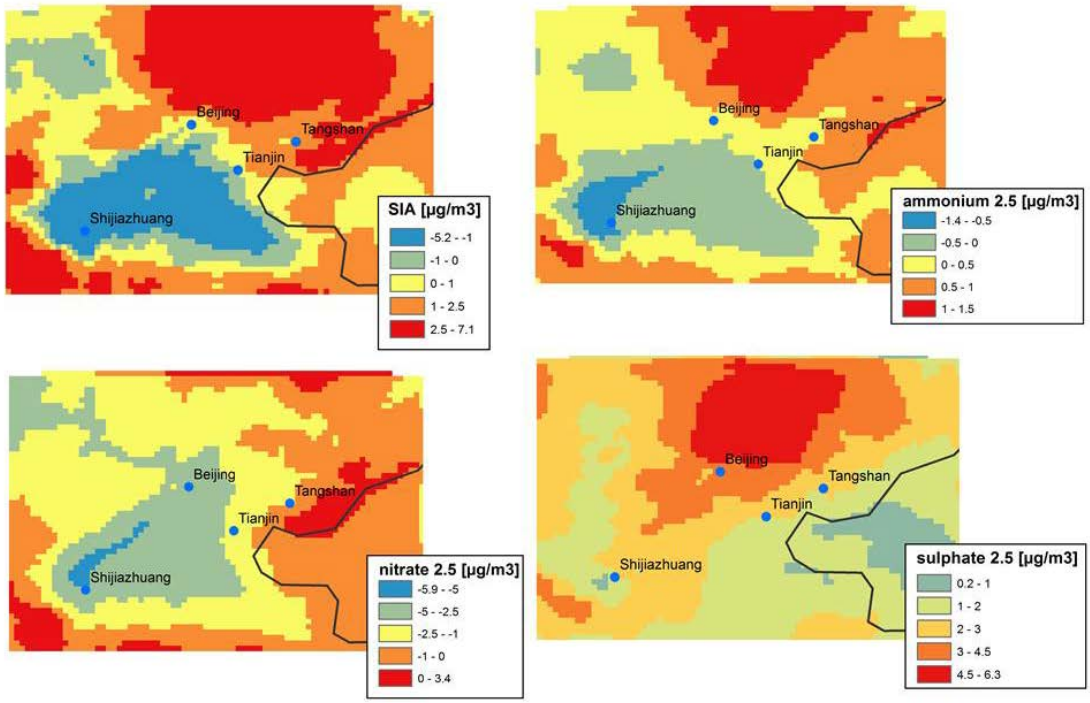

Figure 38. Change in different inorganic aerosol species between the reference and the scenario run: secondary inorganic aerosol (SIA, upper left) and its constituents: ammonium 2.5 (upper right), nitrate 2.5 (lower left) and sulphate 2.5 (lower right).

ANNEXES (ARTICLES, PRESENTATIONS, MISSION REPORTS)

ANNEXE 1. ARTICLES

Published

1. Bauwens, M. J.-F. Müller, T. Stavrakou, J.-F. Müller, I. De Smedt, and M. Van Roozendael, *Satellite-based isoprene emission estimates (2007-2012) from the GlobEmission project*, Proceedings of the ACCENT-Plus Symposium, Atmospheric Composition Change - Policy Support and Science, Urbino, 17-20 September, 2013.
2. De Smedt, I., M. Van Roozendael, T. Stavrakou, J.-F. Müller, C. Lerot, N. Theys, P. Valks, N. Hao, and R. van der A, *Improved retrieval of global tropospheric formaldehyde columns from GOME-2/MetOp-A addressing noise reduction and instrumental degradation issues*, Atmos. Meas. Tech., 5, 2933-2949, 2013
3. De Smedt, M. Van Roozendael, T. Stavrakou, J.-F. Müller, *Intercomparison of five years of global formaldehyde observations from the GOME-2 and OMI sensors*, Proceedings of the ESA Atmospheric Science Conference, Advances in Atmospheric Science and Applications, Bruges, June 2012.
4. Hendrick, F., J.-F. Müller, K. Clémer, P. Wang, M. De Mazière, C. Fayt, C. Gielen, C. Hermans, J. Z. Ma, G. Pinardi, T. Stavrakou, T. Vlemmix, and M. Van Roozendael, *Four years of ground-based MAX-DOAS observations of HONO and NO_2 in the Beijing area*, Atmos. Chem. Phys., 14, 765-781, 2014.
5. Müller, J.-F., J. Peeters, and T. Stavrakou, *Fast photolysis of carbonyl nitrates from isoprene*, Atmos. Chem. Phys., 14, 2497-2508, 2014.
6. Pinardi, G., Van Roozendael, M., Abuhassan, N., Adams, C., Cede, A., Clémer, K., Fayt, C., Friess, U., Gil Ojeda, M., Herman, J., Hermans, C., et al*., MAX-DOAS formaldehyde slant column measurements during CINDI: intercomparison and analysis improvement*, Atmos. Meas. Tech., 6(1), 167–185, 2013.
7. Stavrakou, T., J.-F. Müller, K-F. Boersma, R.J. van der A, J. Kurokawa, T. Ohara, and Q. Zhang, *Key chemical NOx sink uncertainties and how they influence top-down emissions of nitrogen oxides*, Atmos. Chem. Phys. Discuss.. 13, 7871-7929, 2013.
8. Stavrakou, T., J.-F. Müller, A. Guenther, M. Bauwens, I. De Smedt, M. Van Roozendael, A. Guenther, M. Wild, and X. Xia, *Isoprene emissions in Asia over 1979-2012 : impact of climate and land use changes, accepted in* Atmos. Chem. Phys. 2014.
9. Wang, T., F. Hendrick, P. Wang, G. Tang, K. Clémer, H. Yu, C. Fayt, C. Hermans, C. Gielen, G. Pinardi, N. Theys, H. Brenot, and M. Van Roozendael, *Evaluation of tropospheric SO_2 retrieved from MAX-DOAS measurements in Xianghe, China,* Atmos. Chem. Phys. Discuss., 14, 6501-6536, 2014.

In preparation

1. De Smedt, I., T. Stavrakou, T. Danckaert, N. Theys, C. Lerot, J.-F. Müller and M. Van Roozendael, *Satellite observation of tropospheric formaldehyde combining GOME-2 and OMI measurements*, to be submitted to Atm. Meas. Techn., 2014.

2. Gielen, C., M. Van Roozendael, F. Hendrick, C. Fayt, C. Hermans, G. Pinardi, T. Vlemmix, D. Gillotay, V. De Bock, and H. De Backer, *The impact of cloud screening in MAX-DOAS aerosol retrievals*, to be submitted in Atmos. Meas. Tech.

3. Vlemmix, T., F. Hendrick, G. Pinardi, I. De Smedt, C. Fayt, C. Hermans, P. Levelt, and M. Van Roozendael, *MAX-DOAS observations of aerosols, formaldehyde and nitrogen dioxide in the Beijing area: comparison of two profile retrieval approaches*, to be submitted in Atmos. Chem. Phys.

ANNEXE 2. PRESENTATIONS IN WORKSHOPS AND CONFERENCES

Invited presentations

1. Stavrakou, T., J.-F. Müller, J. Peeters, I. De Smedt, M. Van Roozendael, J. Peeters, F. Boersma, and R. van der A, *How do chemical uncertainties affect satellite-derived NOx and VOC emisison estimates?* 2013 China Emissions Workshop, Beijing, 26-27 June 2013.

2. Stavrakou, T., J.-F. Müller, I. De Smedt, M. Van Roozendael, J. Peeters, F. Boersma, and R. van der A, *Addressing the role of major chemical uncertainties on top-down NOx and VOC emission estimates,* PRESCRIBE Workshop, Bremen, 15-16 May 2013.

3. Stavrakou, T., J.-F. Müller, R. van der A, F. Boersma, *Tying down key chemical NOx uncertainties to better constrain long-term global NOx emission estimates and trends inferred from space observations,* AGU Fall Meeting, San Francisco, December 2012.

4. De Smedt, I., M. Van Roozendael, T. Stavrakou, and J.-F. Müller, *Long-term global observations of tropospheric formaldehyde retrieved from spaceborne nadir UV sensors*, AMS meeting: 30th conference on agricultural and forest meteorology/first conference on atmospheric Biogeosciences, Boston, US, 31 May 2012.

Oral presentations

1. IBBAC Progress Meeting, 3 presentations given by M. Van Roozendael, J.-F. Muller, T. Stavrakou (BIRA-IASB) and Peter Viaene (VITO). The presentations are accessible via http://tropo.aeronomie.be/ibbac/documents.htm (login : IBBAC, key : IBBACusers), Institute of Atmospheric Physics (IAP-CAS), of Beijing on September 20, 2012.

2. Hendrick, F., J.-F. Müller, M. De Mazière, C. Fayt, C. Hermans, T. Stavrakou, P. Wang, and M. Van Roozendael, *Four Years of Ground-based MAX-DOAS Observations of HONO and NO2 in the Beijing Area*, EGU Conference, Vienna, 7-12 April 2013.

3. Müller, J.-F., T. Stavrakou, A. Guenther, Jian-Hui Bai, *Long-term historical inventory of isoprene emissions over Asia : interannual variability, trends and evaluation against flux measurements*, poster presented at the IGAC Conference in Beijing, 17-21 September 2012.

4. De Smedt, I., T. Danckaert, C. Lerot, M. Van Roozendael, T. Stavrakou, J.-F. Müller, F. Boersma, P. Veefkind, *Distribution and trends of natural and anthropogenic VOC emissions using OMI/Aura HCHO measurements*, ESA Living Planet Symposium, Edinburgh, 9-13 September 2013.

5. De Smedt, M. Van Roozendael, I., T. Danckaert, T. Stavrakou, and J. Müller, *Formaldehyde diurnal variation as observed with GOME-2 and OMI, ground-based measurements and model simulations*, DOAS workshop, Boulder, US, August 2013.
6. Stavrakou, T., J.-F. Müller, I. De Smedt, M. Van Roozendael, and A. Guenther, *Isoprene emissions in Asia 1979-2012 : variability and trends, effects of changes in meteorology and land use, and comparison with top-down estimates*, ACCENT+ Symposium, Urbino, 17-20 September 2013.
7. De Smedt, I. and M. Van Roozendael: *S5P-TROPOMI HCHO*, talk at First S5P-TROPOMI L2WG Meeting, KNMI, De Bilt, 9-10 July 2012.

Poster presentations

1. Müller, J.-F., T. Stavrakou, A. Guenther, Jian-Hui Bai, *Long-term historical inventory of isoprene emissions over Asia : interannual variability, trends and evaluation against flux measurements*, poster presented at the IGAC Conference in Beijing, 17-21 September 2012.
2. Yu, H., M. Van Roozendael, P. Wang, I. De Smedt, J. van Gent, R. van der A, F. Boersma, P. Valks, A. Richter, T. Stavrakou, and J.-F. Müller, *Intercomparison of tropospheric NO2 retrievals from the OMI and GOME-2 sensors over China*, ESA Living Planet Symposium, Edinburgh, 9-13 September 2013.
3. De Smedt I., Tim Vlemmix, Thomas Danckaert, François Hendrik, Trissevgeni Stavrakou, Jean-François Müller, Gaia Pinardi, Huan Yu, Michel Van Roozendael, *New Harmonised Formaldehyde Retrievals from GOME-2 and OMI and their comparison with MAX-DOAS observations in the Beijing area*, ACVE meeting, ESRIN, Italy, March 2013.
4. De Smedt, I., M. Van Roozendael, T. Stavrakou, J.-F. Müller, K. Chance, and T. Kurosu, *Intercomparison of 4 Years of Global Formaldehyde Observations from the GOME-2 and OMI sensors*, poster at ESA-ATMOS Atmospheric Science Conference, Bruges, Belgium, June 2012.

ANNEXE 3. MISSION REPORTS

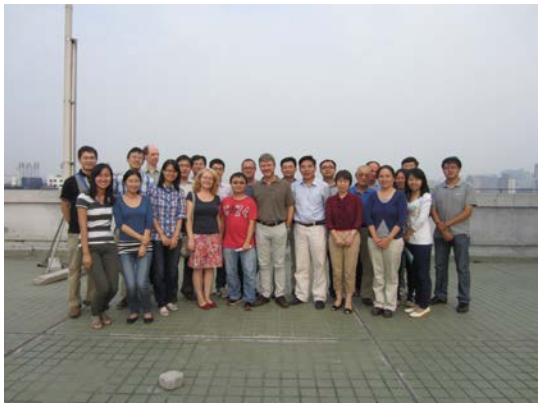

The IBBAC Progress Meeting was held at the Institute of Atmospheric Physics (IAP-CAS), of Beijing on September 20, 2012. A very cordial welcome to the Belgian participants has been given from the Chinese partners, and their interest to attend this meeting was evidenced by the large number of participants (24). More specifically, the meeting was attended by 5 participants from the Belgian side, professors from IAP-CAS, from Peking and Tsinghua University (PKU, THU), from the Chinese Academy of Sciences (CASHIPS), as well as their co-workers. In total, 11 oral presentations have been given, on MAX-DOAS measurements, bottom-up inventories in China for anthropogenic and biogenic emissions, and satellite-derived emissions using inverse modelling techniques. Possibilities to continue the

current synergies, extend and reinforce them in the future have been also discussed during the meeting. The agenda can be found here : (access restricted to IBBAC partners and funding agencies using login: IBBAC password: IBBACusers):

http://tropo.aeronomie.be/ibbac/IBBAC_PM1_Agenda.pdf

and the presentations of all speakers can be reached through

http://tropo.aeronomie.be/ibbac/documents.htm

with in addition, on the same website a poster presented at the IGAC Conference in Beijing (17-21 September 2012) on "Long-term historical inventory of isoprene emissions over Asia : interannual variability, trends and evaluation against flux measurements", by J.-F. Müller, T. Stavrakou, A. Guenther, and J. Bai, is available for download.

ANNEXE 4. PROJECT-RELATED WORKSHOPS

- *PRESCRIBE Workshop, Bremen, Germany, 15-16 May 2013*
  Invited presentation : "Addressing the role of major chemical uncertainties on top-down NOx and VOC emission estimates", T. Stavrakou, J.-F. Muller, I. De Smedt, M. Van Roozendael, J. Peeters, F. Boersma, and R. van der A

- *GSAG 49, EUMETSAT, Darmstadt, Germany, 25 April 2013*
  Oral presentation : "GOME-2 A/B Scientific trace gas retrievals", M. van Roozendael, I. De Smedt, C. Lerot, and H. Yu

- *S5P-TROPOMI Verification Workshop, DLR, Germany, 14-15 April 2013*
  Oral presentation : "S5P-TROPOMI HCHO", I. De Smedt, M. van Roozendael, T. Danckaert, C. Fayt, N. Theys, and J. van Gent

- *EGU Meeting, Vienna, 7-12 April 2013*
  Oral presentation : "Four Years of Ground-based MAX-DOAS Observations of HONO and NO2 in the Beijing Area", F. Hendrick, J.-F. Müller, M. De Mazière, C. Fayt, C. Hermans, T. Stavrakou, P. Wang, and M. Van Roozendael
  Poster : "Analysis on the Characteristics of Tropospheric NO2 in Xianghe from MAX-DOAS Measurement", T. Wang, P. Wang, M. Van Roozendael, and H. Yu

- *O3M SAF CDOP-2 PT Meeting, Brussels, 20-21 March 2013*
  Oral presentation : " GOME-2 MetOp-B trace gases analysis: first results", I. De Smedt, C. Lerot, and M. Van Roozendael

- *Atmospheric Composition Validation and Evolution Workshop, 13-15 March 2013*
  Poster : "New harmonised formaldehyde retrievals from GOME-2 and OMI and their comparison with MAX-DOAS observations in the Beijing area", I. De Smedt, T. Danckaert, T. Vlemmix, F. Hendrik, T. Stavrakou, J.-F. Müller, G. Pinardi, H. Yu, and M. Van Roozendael

- *AGU Fall Meeting, San Francisco, 7-11 December 2012*
  Invited presentation : " Tying down key chemical NOx uncertainties to better constrain long-term global NOx emission estimates and trends inferred from space observations", T. Stavrakou, J.-F. Müller, R. van der A, F. Boersma